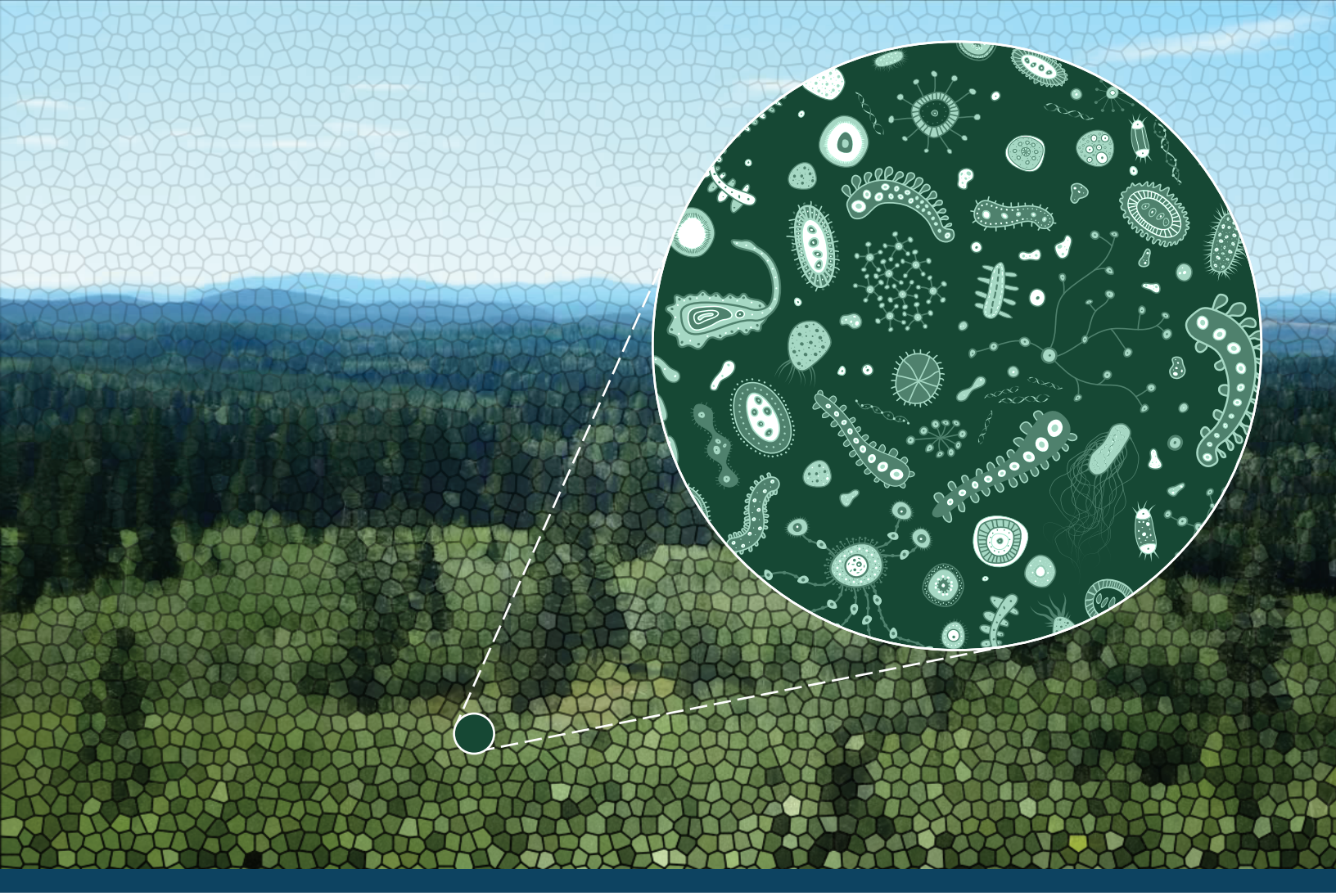

Microbial-Community Fingerprints as Indicators for Buried Mineralization, in British Columbia

Rachel L. Simister, Bianca P. Iulianella Phillips, Peter A. Winterburn, and Sean A. Crowe

Geoscience BC Report 2020-03

MDRU Publication 446

Geoscience BC

MDRU
MINERAL DEPOSIT RESEARCH UNIT

UBC THE UNIVERSITY OF BRITISH COLUMBIA

Microbial-Community Fingerprints as Indicators for Buried Mineralization, in British Columbia

Rachel L. Simister[1], Bianca P. Iulianella Phillips[2], Peter A. Winterburn[2], and Sean A. Crowe[3]

Geoscience BC* Report 2020-03

MDRU Publication 446

[1] Department of Microbiology and Immunology, The University of British Columbia, Vancouver, BC, rlsimister@gmail.com

[2] MDRU–Mineral Deposit Research Unit, Department of Earth, Ocean and Atmospheric Sciences, The University of British Columbia, Vancouver, BC

[3] Departments of Microbiology and Immunology, and Department of Earth, Ocean and Atmospheric Sciences, The University of British Columbia, Vancouver, BC

Keywords: microbial community, DNA sequencing, mineral exploration, British Columbia

Suggested Citation:

Simister, R.L., Iulianella Phillips, B.P., Winterburn, P.A., and S.A. Crowe (2020) Microbial-community fingerprints as indicators for buried mineralization, in British Columbia. Geoscience BC Report 2020-03, MDRU Publication 446, 31 p.

Report prepared by MDRU†

Department of Earth, Ocean and Atmospheric Sciences
The University of British Columbia
Vancouver, BC V6T 1Z4, Canada
Tel: +1-604-822-6136
Email: mdru@eoas.ubc.ca

Includes bibliographic references.
Electronic monograph issued in PDF format.
ISBN 978-0-88865-408-3

*Geoscience BC is an independent, non-profit organization that generates earth science in collaboration with First Nations, local communities, government, academia and the resource sector. Our independent earth science enables informed resource management decisions and attracts investment and jobs. Geoscience BC gratefully acknowledges the financial support of the Province of British Columbia.

†MDRU–Mineral Deposit Research Unit is an internationally-recognized collaborative venture between the mining industry and Earth, Ocean and Atmospheric Sciences Department at The University of British Columbia (UBC), established with assistance from the Natural Sciences and Engineering Research Council of Canada (NSERC), and devoted to solving mineral exploration-related problems.

Cover image: Typical landscape of central British Columbia with dense forest overlying glacial till. Landscape photograph: Peter Winterburn; bacteria symbols by Dragonartz, CC-BY; composite artwork S. Jenkins

DEDICATION

Peter Winterburn will be remembered as a driving force for innovation and exploration geochemistry. His legacy lives on through the influences and the impacts he has made to the discipline. Without the expertise of Peter this research would not have been possible.

ABSTRACT

Microbial communities are acutely sensitive to subtle variability in their surroundings—they respond to and adapt for optimal growth and metabolism across an extremely wide range of chemical conditions. High-throughput DNA sequencing combined with geomicrobiological knowledge has the potential to transform the mineral exploration industry and the way we sense and interact with geologic materials. Here we report the development and application of a DNA sequencing-based mineral exploration technology that leverages soil microbial communities as trillions of in-situ microsensors that collectively detect environmental anomalies linked to buried mineral deposits. Data have been collected from incubation experiments and two field sites located in British Columbia, Canada. Our results show that sequencing of microbial DNA from soils effectively resolves mineralization buried deep below glacial till overburden. We find that sequence-based anomaly detection is both more sensitive and robust than classical geochemical/geophysical methodologies. The ability to harness sequence information from the environment will continue to enhance our interaction with the Earth system and support the growing global bioeconomy.

1. INTRODUCTION

As global population grows and modernizes, demand for mineral resources is rapidly expanding (Kesler 2007; Lusty and Gunn 2015). At the same time, existing mineral deposits are being exhausted and the frequency of new deposit discovery based on outcropping mineralization has declined. New demand for mineral resources must, therefore, be increasingly met through the discovery and development of concealed deposits, many of which are obscured by burial, weathering, erosion, or structural offset (Cameron et al. 2004; Gilliss et al. 2004; Kelley et al. 2006). New and innovative techniques are thus needed to detect trace surface expression of buried mineralization and promote new mineral resource discovery (Kelley et al. 2006). Recent studies have demonstrated the potential of new surface geochemical techniques to promote discovery of concealed orebodies (Townley et al. 2007; Reid et al. 2009; Bissig and Riquelme 2010; Heberlein and Samson 2010; Plouffe et al. 2013a, b; Zhang et al. 2015), however, the geochemical signatures generated from orientation surveys over known deposits are typically noisy with poor anomaly to background resolution (Stanley 2003), have poor reproducibility, and often exhibit element patterns that are difficult to reconcile with mineral-deposit chemistry and known trace-element mobility patterns (Heberlein and Samson 2010). Despite these issues, there is sufficient empirical evidence to indicate causative links between mineralization beneath transported cover and the presence of subtle geochemical gradients in the surface environment (Hamilton 1998; Kelley et al. 2006; Nordstrom 2011). Although much less examined than geochemical element indicators, biological anomalies may provide more robust indicators of buried mineralization, and such anomalies may be detectable through low-cost, high-throughput geobiological surveys (Kelley et al. 2006).

Micro-organisms kinetically enhance and exploit thermodynamically favorable geochemical reactions, including the dissolution and formation of diverse minerals, to support their metabolism and growth in nearly every low-temperature geological setting (Newman and Banfield 2002; Falkowski et al. 2008). They are acutely sensitive and rapidly respond to dynamics of chemical and physical gradients in the environment. Subtle changes in mineral bioavailability, for example, can be reflected in dramatic shifts in composition and activity of microbial communities (Fierer 2017). Microbial community profiles thus have strong potential to resolve chemical and physical differences in sample suites that are not readily discernible through conventional geochemical and geophysical surveys. The advent of high-throughput next-generation sequencing (NGS) platforms over the last decade has transformed the capacity to interrogate diverse microbial communities in natural and engineered ecosystems (Binladen et al. 2007; Zhou et al. 2015). Application of NGS technologies allows profiling of the taxonomic diversity and metabolic potential of soil microbial communities across defined survey areas. Given that each soil sample comprises thousands of microbial taxa, each containing hundreds to thousands of genes sensing and interacting with the surrounding soil environment (Fierer 2017), the statistical power of this approach to identify anomalies is unprecedented.

British Columbia (BC) is host to numerous mineral deposits of economic value, including a wealth of Cu-porphyry mineralization, however, discovery success from outcrops has declined (Anderson et al. 2012; Ferbey et al. 2014). Mineral deposits in many parts of the province are likely overlain by young (<12 000 years) glacial overburden, making new discoveries challenging. Successful exploration for these deposits is dependent on technologies that can detect mineralization through glacial overburden. British Columbia is an ideal region to evaluate microbial-community sequencing as an exploration methodology for 'seeing' through overburden, as multiple field sites can be tested. Here we show in lab incubations and at multiple field sites that soil microbial-community fingerprinting using modern DNA sequencing technologies can be employed to find buried mineralization. The strong microbial responses observed are encouraging signs for the use of microbial-community fingerprinting in mineral-deposit exploration.

1.1 Project Goal

The primary goal of this project was to test whether high-throughput sequencing technologies can enable the use of soil microbial community profiling as a robust, efficient, and cost-effective tool to identify and locate buried mineral deposits

1.2 Project Scope

Lab incubations were used to enhance our ability to recognize microbial fingerprints in the surface environment related to buried mineralization. The incubations were initiated by adding ("amending") chalcopyrite ore or copper sulfate solutions to "background soils" and measuring the microbial community response. Two field sites were then evaluated to test the use of microbial-community fingerprinting in mineral deposit exploration (Figure 1a);

1) The Deerhorn Cu-Au porphyry deposit (MINFILE 093A 269; BC Geological Survey, 2015) located 70 km northeast of Williams Lake is one of at least five undeveloped porphyry systems that form the Woodjam Projects, which is currently being explored by Consolidated Woodjam Copper Corp. (and previously by Gold Fields Horsefly Exploration Corp.); and

2) The Highmont South Cu-Mo porphyry deposit (MINFILE 092ISE013; BC Geological Survey, 2015) is part of the Highland Valley Copper (HVC) system in south-central BC, which is currently operated by Teck Resources Limited ("Teck").

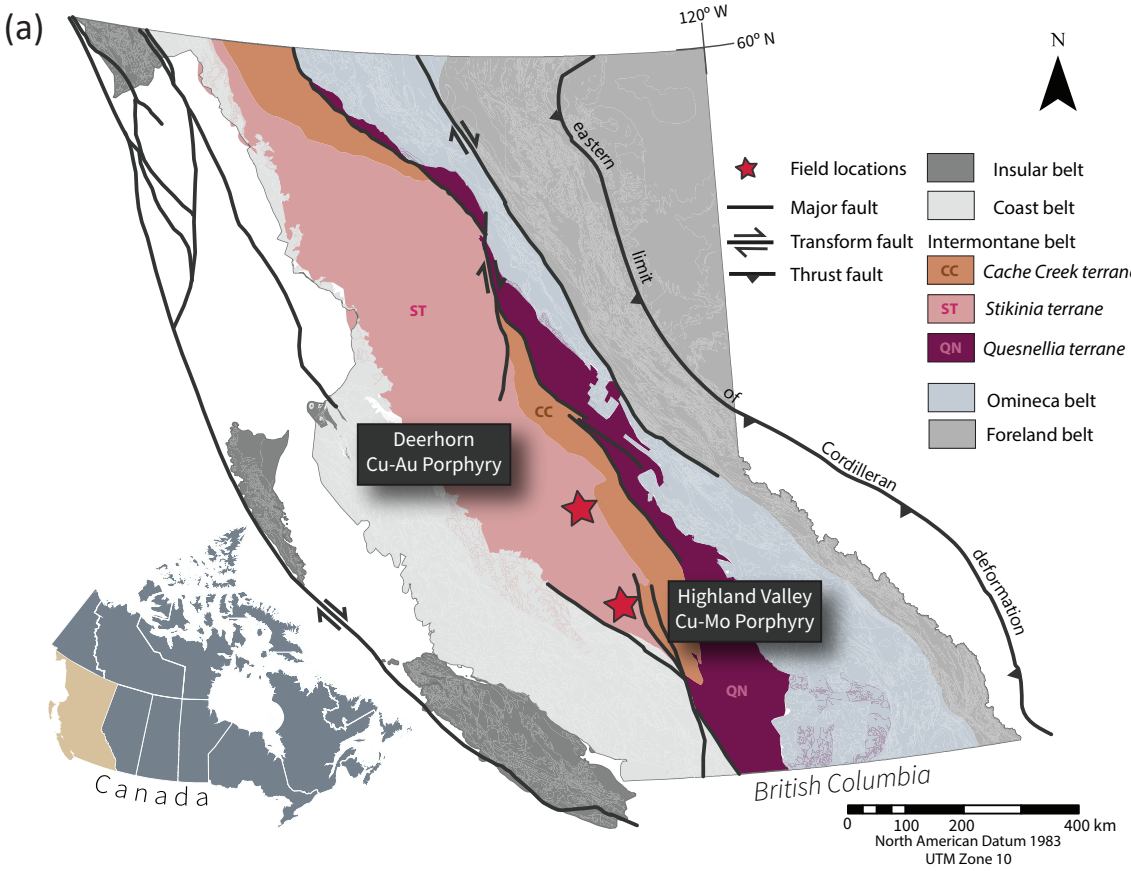

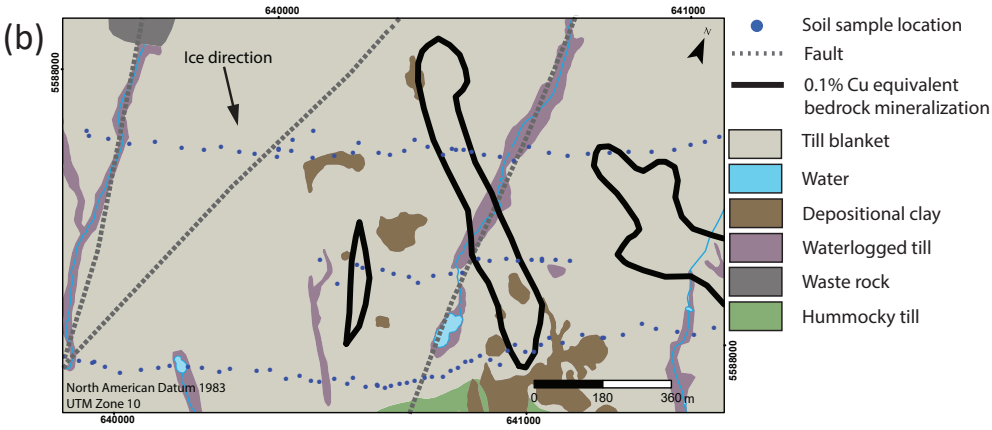

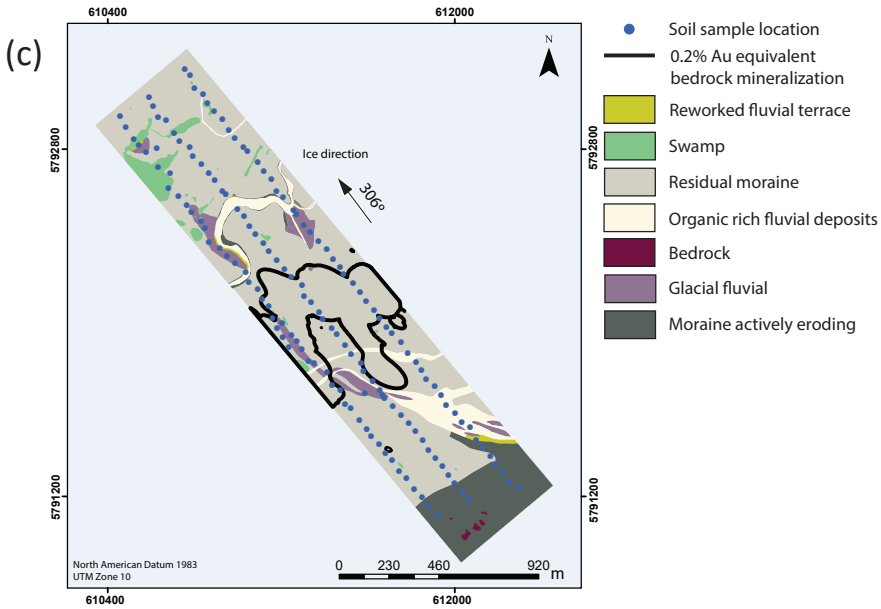

Figure 1: (a) Simplified geologic map of British Columbia organized based on geologic belts of the Canadian Cordillera. The dominant terranes that make up the Intermontane belt—host to the Highmont South and Deerhorn porphyry deposits—are highlighted: pink, orange, and purple to represent the Stikinia terrane, Cache creek terrane, and Quesnellia terrane, respectively. The locations of Highland Valley and Deerhorn are indicated with red stars. Thick black lines indicate major faults. Terranes and geologic belts are characterized based on bedrock mapping carried out by the British Columbia Geological Survey (BCGS) (Open File 2017-8, 9p, data version 2019-12-19: Cui et al. (2017)); **(b)** Map of the Highmont South Cu-Mo porphyry copper deposit with soil sample sites shown as blue dots. Surface projection of bedrock mineralization is indicated by 0.1% copper equivalent. Map units are based on surficial mapping by Chouinard (2018) and Plouffe and Ferbey (2015); **(c)** Map of the Deerhorn Cu-Au porphyry copper deposit with sample soil sites shown as blue dots. Surface projection of bedrock mineralization is indicated by 0.2% gold equivalent. Map units are based on surficial mapping described in Rich (2016).

Geochemical data for the Deerhorn deposit was originally reported by Rich and Winterburn (2016) in Geoscience BC, Report 2016-1, p. 167–174, (also Rich 2016) and geochemical data for HVC deposit was originally reported by Chouinard et al. (2017) in Geoscience BC, Report 2016-1, p. 125–132 (also Chouinard 2018). This report will build upon these earlier studies to evaluate whether microbial communities in soil can be used as an exploration tool to detect mineralization.

2. MATERIALS AND METHODS

2.1 Field locations

Sampling for geochemical and microbiological analysis was completed in July 2015 for both the Deerhorn Cu-Au porphyry and the Highland Valley Copper (HVC) Highmont South Cu-Mo porphyry. The HVC mineralization is expressed in a gradational change from Cu-sulphide-rich minerals in the centre (bornite, chalcopyrite) to a primarily Fe-sulphide (pyrite only)-rich outer zone (Chouinard 2018) with an average till thickness above mineralization of 5 m. The HVC sampling program, consisting of three transects (Figure 1b) perpendicular to the main mineralized zones (0.1% Cu equivalent) in the Highmont South region was conducted over two separate field surveys. Sample sites were selective, as the till in the region was variable, with changes in vegetation, anthropogenic influences and areas that have been appreciably waterlogged (Chouinard 2018). The Deerhorn survey consisted of three transects across subsurface mineralization (Figure 1c), with overlying glacial sediments ranging from 10 to 60 m in thickness and an extremely variable surficial environment with respect to regolith and vegetation (Rich and Winterburn 2016). Mineralization is hosted primarily in monzonite intrusions as disseminated and vein-hosted Cu and Au, with the main zone of mineralization located beneath thick glacial overburden (Rich and Winterburn 2016). For both field locations, soils for microbial community profiling (200 g) were collected aseptically with sanitized equipment and frozen upon return to the lab after 1-2 weeks, prior to DNA extraction and PCR sequencing. Soils for geochemical analyses (~1 kg) were field sieved to -180 µm and sent to ALS Minerals Laboratories (North Vancouver, BC) for aqua-regia digestion and inductively coupled plasma–mass spectrometry (ICP-MS) analysis. Field duplicates, CRMs (certified reference materials), and blanks were inserted into the analytical stream every 15 samples.

2.2 Incubation experiments

For the incubation experiment, one (5 kg) soil sample from close to the Deerhorn Porphyry was retrieved and stored in the dark at ambient temperature (~21°C) until use. The sample was collected from the upper B-horizon under aseptic conditions and screened to -6mm in the field prior to storage at ambient temperatures in double-sealed Ziploc® bags. The soil was not dried prior to the start of the incubation experiment. This sample is considered as representative of background soil if its geochemical indicator and pathfinder elements are below the anomalous threshold determined statistically for the surveyed area. Therefore ~2 g of subsample of the soil was digested using an aqua-regia near total digestion and the digestate was analyzed by ICP-MS to determine that the soil contains 6 ppm Cu, 1 ppm As and 0.32 ppm Mo. Soil (~150 g) was dispensed aseptically into sterile containers for each treatment, and each container was amended with concentrations chosen to represent either concentrations of copper that are routinely detected in geochemical surveys over buried mineral deposits (ambient or '(Amb)') or very high levels of copper that might be expected in highly anomalous soils ('high'). The amendments were as follows:

1) 'High-ore' soil was created by amending the soil with chalcopyrite at a grade of 600 ppm Cu;

2) 'Amb-ore' soil was created by amending the soil with chalcopyrite at a grade of 200 ppm Cu;

3) 'High-Cu' soil was created by amending the soil with copper in the form of $CuSO_4$ (dissolved in Milli-Q®-filtered water) to 600 ppm Cu; and

4) 'Amb-Cu' soil was created by amending the soil with copper in the form of $CuSO_4$ to 200 ppm Cu.

Chalcopyrite ore was crushed to 100% (<70 microns), to ensure even amounts could be added to each soil sample. Soils were kept in the dark, at ambient room temperature (~21°C) under aerobic conditions. Sample containers were parafilmed to prevent moisture loss. The amended soils were then subsampled (2g) for microbial analysis at T = 0, T = 1 (14 days) and T = 2 (35 days). Soil subsamples were kept frozen at -80°C until microbiological analysis (see section 2.3).

In order to see if microbial communities from a different soil type would respond to ore amendment, a second incubation experiment was run using soil located from the Northwest Territories (NWT) (Wickham 2019). Soil samples with background-level metal concentrations were collected from the upper B-horizon under aseptic conditions. Soils were field screened to 6 mm and packed into double Ziploc® sample bags and stored at ambient temperature (15°C) in the field, in the dark until use in the experiment. The bulk soil was not dried prior to the start of the experiment. This sample is considered as representative of background soil if its geochemical indicator and pathfinder elements are below the anomalous threshold determined statistically for the surveyed area. Therefore ~2 g of subsample of the soil was digested using a multi-acid digestion and the digestate was analyzed by ICP-MS at ALS Minerals Laboratories Ltd. (North Vancouver, BC) to determine that the soil contains 10 ppm Cu, 2 ppm As, 0.04 Ag ppm and 10 ppm Pb. Soil was then dispensed aseptically into sterile containers for each treatment and amended with the same chalcopyrite ore described above at

200 ppm but this time with three replicates per treatment. The amended soils were then sampled over a longer time scale than in the first incubation, at T = 0, T = 1 (15 days) and T = 2 (55 days) and T=3 (85 days). Soils were kept in the dark, at ambient room temperature (~21°C) under aerobic conditions. Sample containers were parafilmed to prevent moisture loss. The amended soils were then subsampled (2 g) for microbial analysis at T = 0, T = 1 (14 days) and T = 2 (35 days). Soil subsamples were kept frozen at -80°C until microbiological analysis (see section 2.3).

2.3 DNA extraction, quantification and quality assessment

DNA was extracted using a DNeasy PowerSoil Kit (Qiagen) as per manufacturer's instructions. Resulting DNA was stored at -20°C. Quantification was conducted using the PicoGreen® Assay (Invitrogen) for dsDNA (Singer, Jones et al. 1997), measured on a TECAN™ M200 (excitation at 480 nm and emission at 520 nm). Purity and quality of DNA was assessed based on ratios for A260/A280 measured using a NanoDrop® ND-1000 spectrophotometer (Thermo Scientific). DNA absorbs light of the wavelength 260 nm. The concentration of pure double-stranded DNA with an A260 of 1.0 is 50 mg/ml, and pure nucleic acids typically yield a 260/280 ratio of ~1.8 for DNA.

2.4 SSU rRNA gene amplification and iTag sequencing

Bacterial and archaeal small subunit ribosomal (SSU rRNA) gene fragments (V4 region) were amplified from the extracted genomic DNA. This gene fragment is used for microbial community analysis as it is present in all bacterial and archaeal species. Sample preparation for amplicon sequencing was performed as described by Caporaso et al. (2011) and Apprill et al. (2015). In brief, the aforementioned SSU rRNA gene-targeting primers, complete with Illumina adapter, an 8 nucleotide (nt) index sequence, a 10-nt pad sequence, a 2-nt linker and the gene specific primer were used in equimolar concentrations together with deoxyribonucleotide triphosphate (dNTPs), Polymerase chain reaction (PCR) buffer, MgCl, 2U/ul ThermoFisher Phusion Hot Start II DNA polymerase and PCR-certified water to a final volume of 25 µL. PCR amplification was performed with an initial denaturing step of 95°C for 2 min, followed by 30 cycles of denaturation (95°C for 20 s), annealing (55°C for 15 s), and elongation (72°C for 5 min), with a final elongation step at 72°C for 10 min. Chalcopyrite ore added to incubation studies, was also subjected to DNA extraction and PCR, no 16S rRNA amplicons were detected. Equimolar concentrations of prepared amplicon bearing solutions were pooled into a single library by using the Invitrogen SequalPrep™ kit. The amplicon library was analyzed on an Agilent 2100 Bioanalyzer (Agilent Technologies, Inc.) using the High Sensitivity DS DNA assay to determine approximate library fragment size, and to verify library integrity. Pooled library concentration was determined using the KAPA Library Quantification Kit for Illumina. Library pools were diluted to 4 nM and denatured into single strands using fresh 0.2 N NaOH as recommended by Illumina. The final library was loaded at a concentration of 8 pM, with an additional PhiX spike-in of 5–20%. Sequencing was conducted at the University of British Columbia Sequencing and Bioinformatics Consortium (https://sequencing.ubc.ca/).

2.5 Bioinformatic analysis

Genomic Sequences (herein referred to as sequences) were processed using Mothur (Schloss et al. 2009). In brief, sequences were removed from the analysis if they contained ambiguous characters, had homopolymers longer than 8 base-pairs (bp) and did not align to a reference alignment of the correct sequencing region. Unique sequences and their frequency in each sample were identified and then a pre-clustering algorithm was used to further de-noise sequences within each sample (Schloss et al. 2011). Unique sequences were identified and aligned against a SILVA alignment (available online at http://www.mothur.org/wiki/Silva_reference_alignment). Sequences were chimera checked using UCHIME (Edgar et al. 2011) and reads were then clustered into 97% Operationally defined Taxomomic Units (OTUs) using OptiClust (Westcott and Schloss 2017). OTUs were classified using SILVA reference taxonomy database (release 132, available at http://www.mothur.org/wiki/Silva_reference_files). For alpha diversity measures, all samples were subsampled to the lowest coverage depth and calculated in Mothur (Schloss et al. 2009).

3. RESULTS AND DISCUSSION

3.1 Copper incubation experiments

Soil is one of the most complex and diverse microbial habitats, with merely 1 g containing up to 1010 cells and 104 bacterial species (Torsvik and Øvreås 2002; Roesch et al. 2007). This study's approach relies on the ability to capture this diversity through next-generation sequencing technologies. In microbiology, the assessment of diversity often involves calculation of species richness, which is the number of species present in a sample (Magurran 2013). The most common approach is to assign 16S rRNA sequences into operational taxonomic units (OTUs) and represent these as rarefaction curves, which plot the cumulative number of OTUs captured as a function of sampling effort, and therefore indicate the OTU richness in a given set of samples. Other common methods include nonparametric analysis, such as Chao1 (Chao 1984), which estimates the overall sample diversity also known as alpha diversity (Hughes et al. 2001). In the first incubation experiment soil from Deerhorn, British Columbia was amended with either chalcopyrite ore or $CuSO_4$; in the second incubation experiment soil from the Northwest Territories was amended with chalcopyrite ore. In both incubation experiments microbial-community DNA was extracted from the soils and the 16S rRNA gene was sequenced.

Table 1: Chalcopyrite ore and copper sulfate incubation experiment 1 (Deerhorn, BC soil). Overview of the species estimates and diversity metrics obtained per sample after quality filtering. Sample names explained in 'Soil and Ore Incubation' section. Abbreviation: OTU, operational taxonomic unit

Sample ID	# OTUs	Chao1	Inverse Simpson Index
T0 control	2156	3000	69
T0 Amb cu	2321	3318	54
T0 High cu	2387	3371	48
T0 Amb ore	2231	3128	72
T0 High ore	2189	2973	80
T1 control	2315	3331	65
T1 Amb cu	2310	3210	76
T1 High cu	2177	2876	79
T1 Amb ore	2325	3461	72
T1 High ore	2325	3274	69
T2 control	2333	3349	65
T2 Amb cu	2330	3333	66
T2 High cu	2265	3033	72
T2 Amb ore	2305	3524	59
T2 High ore	2237	3054	71

3.1.1 Incubation of Deerhorn, British Columbia (BC) soils amended with either chalcopyrite ore or copper sulfate

Analysis of these sequences reveals that the number of observed OTUs is 2280 ±68 (range 2156–2387), with an alpha diversity Chao1 Index of 3216 ±194 (range 2876–3524), and Inverse Simpson Index of 68 ±9 (range 48-80) (Table 1). By comparing the number of observed OTUs and Chao1 estimates we indicate that the sequencing coverage was sufficient to capture 71% of the microbial-community diversity. These levels of diversity are well in line with diversity commonly observed in soils (Thompson et al. 2017) and dispel dogma that extremely high diversity in soil microbial communities renders them intractable to molecular-based microbial-community analysis. There was no pronounced difference in species richness (i.e., the number of species in a given sample) over time, due to amendment with chalcopyrite ore or copper sulfate. Only in Hi-Ore samples at T2 was there a small increase in species diversity as measured by the Inverse Simpson Index. The study's first measurements demonstrate that soil diversity can be captured through next-generation sequencing technologies, which bodes well for the approach and demonstrates the enormous statistical power in community profiles as potential mineralization indicators.

The number of reads per microbial phylum was normalized to total read number for a given sample and expressed as a percentage of the total reads from that sample (Figure 2a). Most microbial-community members belong to the Proteobacteria (31 ± 4%), Acidobacteria (25 ± 7%), and Verrucomicrobia (18 ± 2.8%) phyla (Figure 2a). The relative proportions are consistent with previous studies on soil ecosystems (Kaiser et al. 2016; Choi et al. 2017). This high-level taxonomic analysis reveals strong similarities across all samples, thus giving confidence that the analyses are not overwhelmed by intersample variability arising because of the combination of very high levels of microbial diversity and the chemical and physical heterogeneity commonly found in soils. The similarity across the samples, however, suggests that differences between background and anomalous soils may only be resolved through analyses at the genus or species level rather than at the phylum level. Nevertheless, when plotted relative to the unamended (control) samples, subtle changes in community composition through time can be detected even at the phylum level. For example, differences between copper sulfate-amended and chalcopyrite ore–amended soils included a higher abundance of Firmicutes in Hi-Ore, Hi-Cu and Amb-Cu treated soils at T1 and T2 (Figure 2b). The phylum Chloroflexi also increased in abundance relative to the control in samples

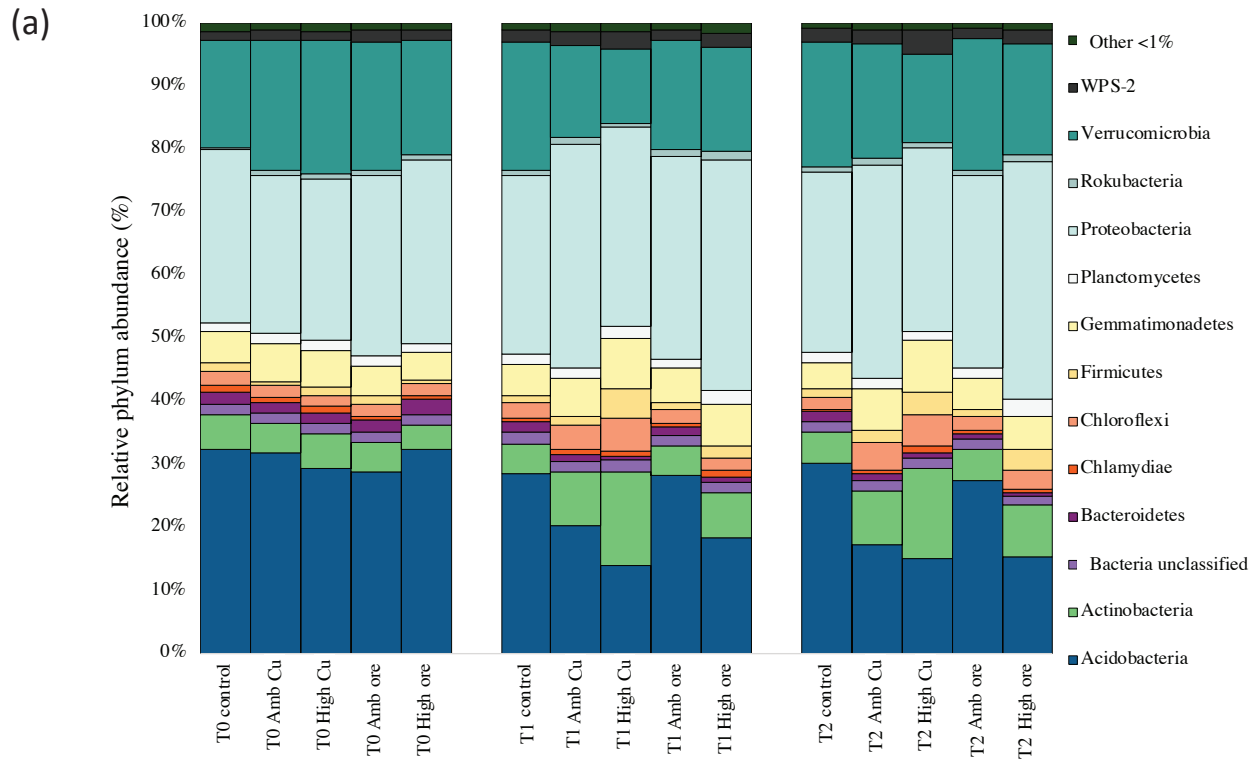
(a)
Relative phylum abundance (%)
100%
90%
80%
70%
60%
50%
40%
30%
20%
10%
0%
T0 control
T0 Amb Cu
T0 High Cu
T0 Amb ore
T0 High ore
T1 control
T1 Amb Cu
T1 High Cu
T1 Amb ore
T1 High ore
T2 control
T2 Amb Cu
T2 High Cu
T2 Amb ore
T2 High ore
Other <1%
WPS-2
Verrucomicrobia
Rokubacteria
Proteobacteria
Planctomycetes
Gemmatimonadetes
Firmicutes
Chloroflexi
Chlamydiae
Bacteroidetes
Bacteria unclassified
Actinobacteria
Acidobacteria

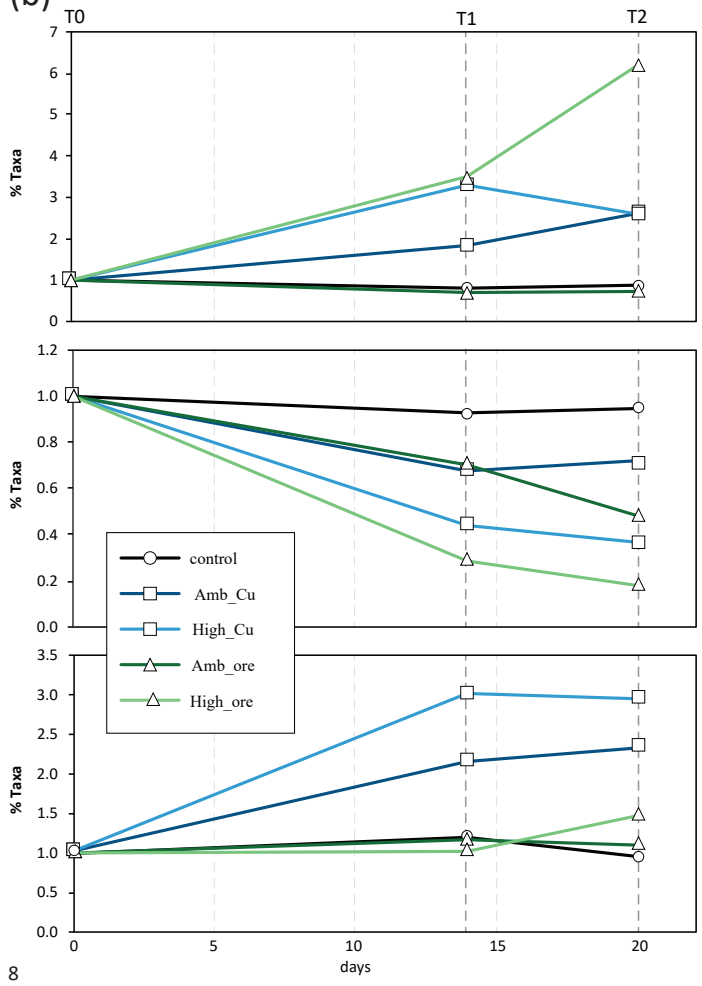
(b)
T0
T1
T2
% Taxa
control
Amb_Cu
High_Cu
Amb_ore
High_ore
days

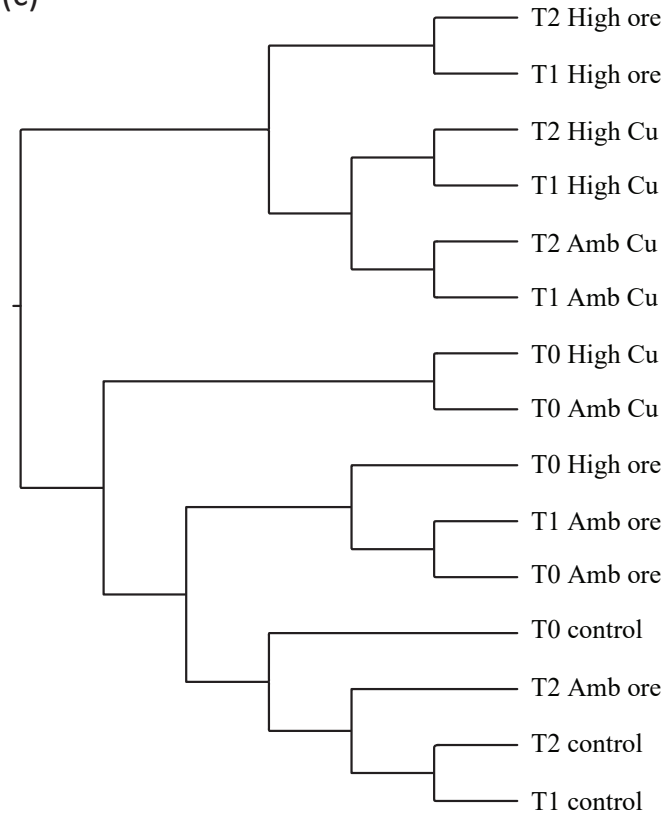
(c)
T2 High ore
T1 High ore
T2 High Cu
T1 High Cu
T2 Amb Cu
T1 Amb Cu
T0 High Cu
T0 Amb Cu
T0 High ore
T1 Amb ore
T0 Amb ore
T0 control
T2 Amb ore
T2 control
T1 control

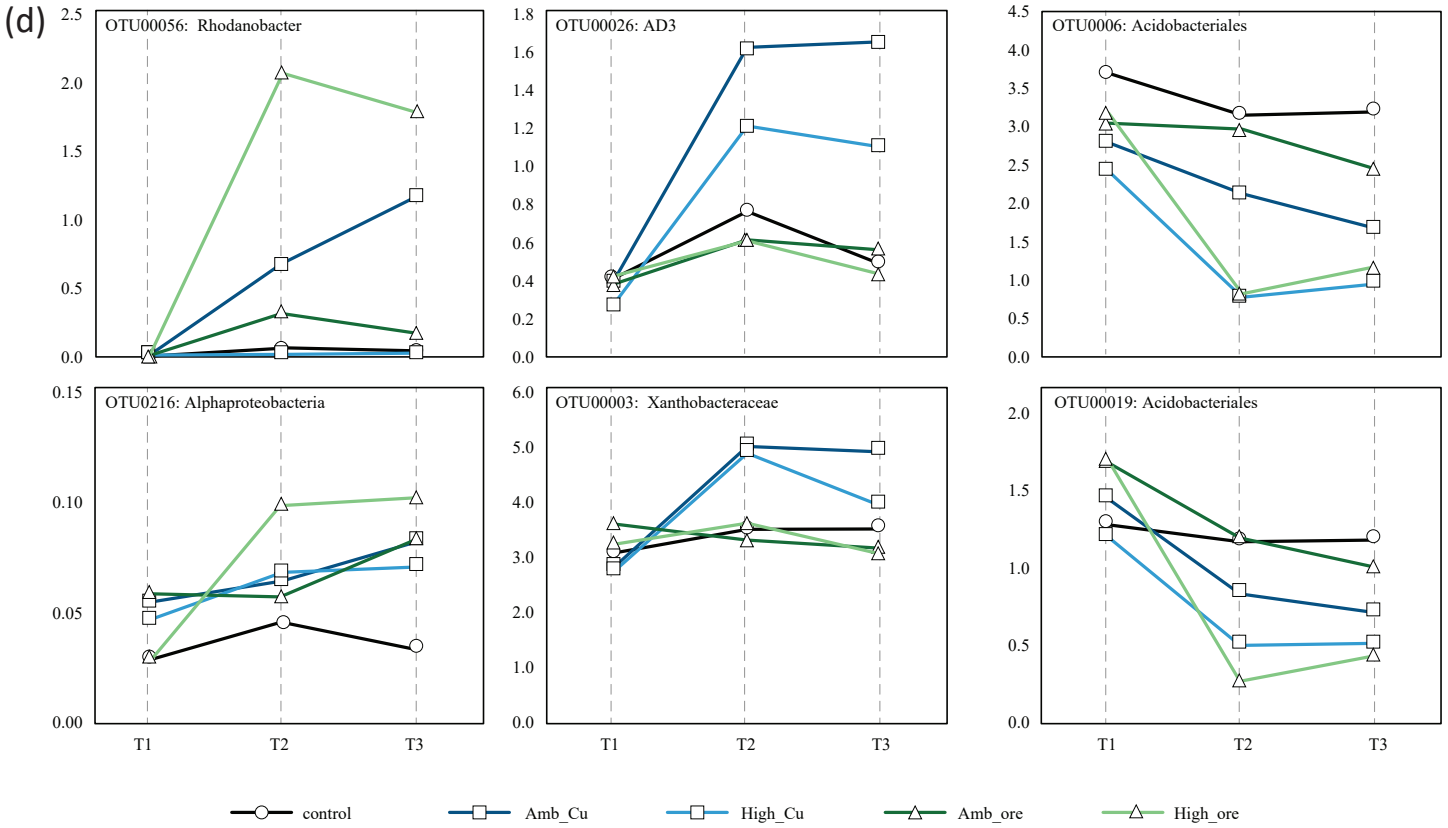

Figure 2: (a) Distribution of 16S rRNA reads per phylum for each sample in the BC soil incubation experiment. The number of reads per phylum is calculated as a percentage of the total reads for each sample. The "other" grouping represents summed phyla that individually contributed <1% of the total number of reads per sample; **(b)** Examples of changes in phylum abundance over time for each sample/treatment. The number of reads per phylum is calculated as a percentage of the total reads for each sample; **(c)** Hierarchical relationships among samples based on the Yue and Clayton similarity distance matrix of 16S-OTU abundances. The hierarchical relationships between samples were obtained using the UPGMA clustering algorithm. Node labels indicate the sample/treatment; **(d)** Examples of operational taxonomic unit (OTU) changes across treatments, over time. In all plots, "T" stands for time point.

amended with ambient and high levels of copper (Amb-Cu and Hi-Cu; Figure 2b). All amendments elicited a decrease in the relative abundance of Bacteroidetes compared to control soil over time (Figure 2b). Relationships between treatment type (chalcopyrite ore or copper sulfate) and time point (T = 0, 1, 2) were evaluated through hierarchical-clustering analysis at the OTU level (Figure 2c). All control samples clustered tightly, confirming similar microbial-community compositions. High and ambient copper sulfate-treated samples as well as high ore-treated samples grouped apart from controls, indicating that chalcopyrite ore and copper sulfate amendments changed the composition of the microbial community and that this change was easily resolvable through standard hierarchical-clustering analysis. Hierarchal clustering separated chalcopyrite ore- and copper sulfate-treated samples, indicating that it may be possible to determine microbial community response to individual metals and/or their mineralogical composition.

To assess whether individual bacterial taxa were significantly different in control soils versus soils amended with ore or copper sulfate, we performed a Linear discriminant analysis effect size (LEfSe analysis) (Segata et al. 2011) on the OTU dataset. Sample groups were set for this analysis based on their origin from "control soil" or "soils amended with ore or copper sulphate". A number of species were significantly (P=<0.05) enriched or depleted in response to chalcopyrite ore or copper sulfate amendment. The relative abundance of individual species normalized to the relative abundance of the same species in the controls was plotted versus time (6 examples (those with largest changes in abundance over time) are shown in Figure 2d). The species that showed a response to chalcopyrite ore and copper sulfate amendment relative to controls included Rhodanobacter sp., Chloroflexi sp AD3., Acidobacteriales sp., and unclassified Alphaproteobacterial species. These species have frequently been found in materials recovered from acidic waters, sulphidic mine wastes, and other mine-related environments, as well as acidic biofilms (Hallberg et al. 2006; Stackebrandt 2014; Koh et al. 2015; Gavrilov et al. 2019), anecdotally suggesting a link between the ecology of these species and the concentration of metals in their habitat. In addition to the broader community-level responses revealed through hierarchical clustering analyses, the data from this study thus imply that certain species in

soil microbial communities may be useful as specific indicators of exposure to ore components.

3.1.2 Incubation of Northwest Territories (NWT) soils amended with chalcopyrite ore

In order to see if different soils would also elicit a response in microbial communities in the presence of weathered ore, we chose to incubate soil from the Northwest Territories (NWT) of Canada. These soils were of lower diversity than soils from BC, with the average number of observed OTUs 784 ± 188 (range 476–1043), with an alpha diversity Chao1 index of 1146 ±276 (range 634-1492), and Inverse Simpson Index of 20 ±14 (range 3-46) (Table 2). Once again sequencing coverage was sufficient to capture most of the microbial-community diversity (68%). Similar to the BC soil incubation the majority of 16S rRNA gene sequences were assigned to Proteobacteria, Actinobacteria, Bacteroidetes, Acidobacteria, Chloroflexi and WPS-2 phyla (Figure 3a), with smaller proportions assigned to the Verrucomicrobia and Planctomycetes (Figure 3a), which are phyla that are ubiquitously found in soil ecosystems globally (Fierer 2017).

Unlike in the BC soil experiment, microbial communities in the NWT soils changed dramatically when amended with chalcopyrite ore. The abundance of Proteobacteria averaged 46% in control and 74% in ore amended soils and they became dominant components of the bacterial community (Figure 3a). Phyla that were abundant in control samples, i.e., Acidobacteria, Actinobacteria, Verrucomicrobia and WPS-2, were present in ore

Table 2: Chalcopyrite ore and copper sulfate incubation experiment 2 (NWT soil). Overview of the species estimates and diversity metrics obtained per sample after quality filtering. Sample names explained in 'Soil and Ore Incubation' section. Abbreviation: OTU, operational taxonomic unit

Sample ID	# OTUs	Chao1	Inverse Simpson Index
T0_control_A	960	1385	37
T0_control_B	1043	1437	46
T0_control_C	935	1357	39
T0_CUAU_A	909	1277	22
T0_CUAU_C	894	1208	27
T1_control_A	994	1492	29
T1_control_B	858	1276	22
T1_control_C	957	1361	34
T1_CUAU_A	476	804	3
T1_CUAU_B	617	1034	4
T1_CUAU_C	675	1101	5
T2_control_A	874	1296	23
T2_control_B	903	1342	29
T2_control_C	933	1414	30
T2_CUAU_A	510	742	4
T2_CUAU_B	543	882	4
T2_CUAU_C	493	634	4
T3_control_A	903	1370	32
T3_control_B	897	1302	31
T3_control_C	880	1330	32
T3_CUAU_A	568	737	5
T3_CUAU_B	580	762	4
T3_CUAU_C	627	817	5

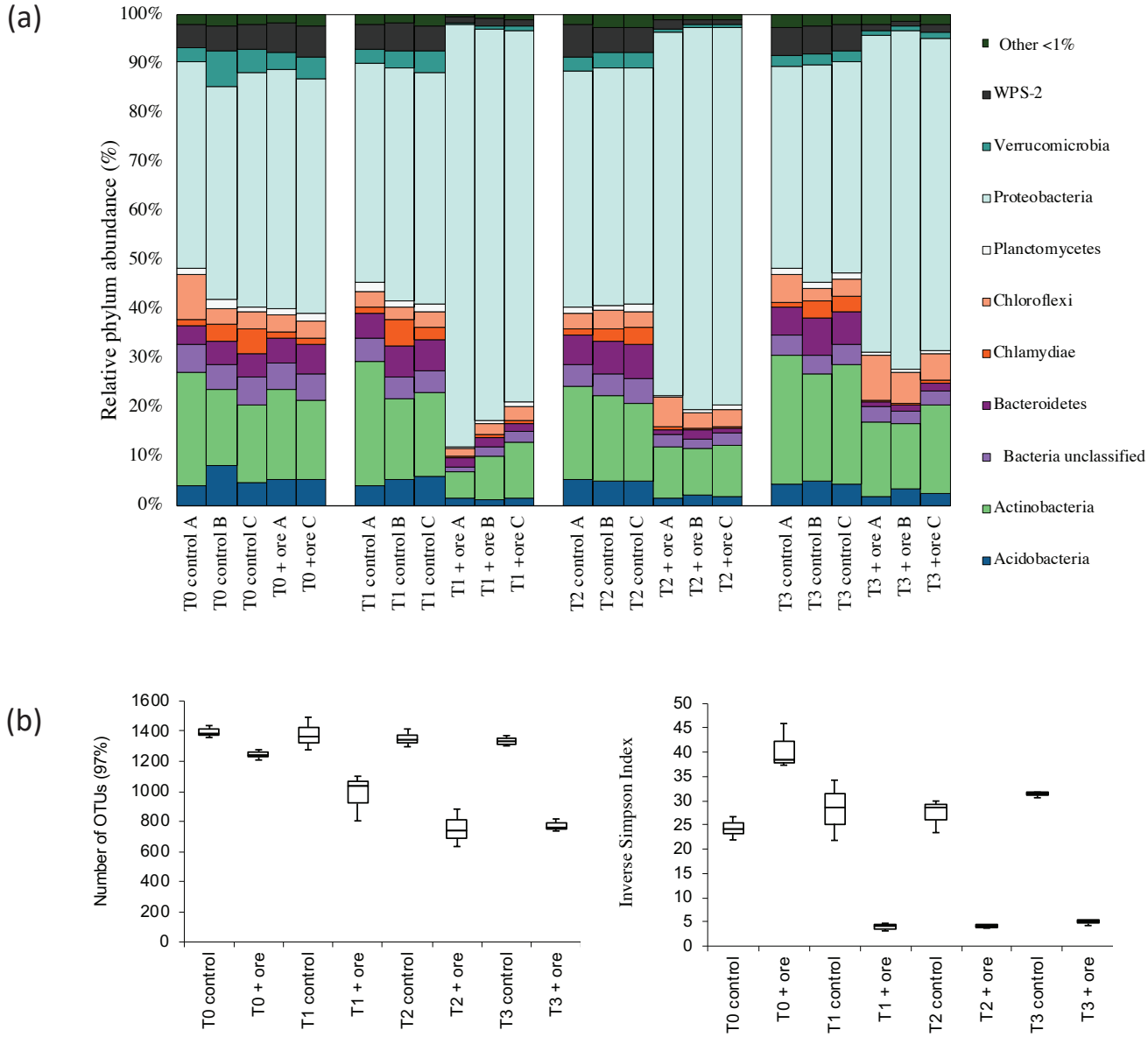

Figure 3: (a) Distribution of 16S rRNA reads per phylum for each sample in the NWT soil incubation experiment. The number of reads per phylum is calculated as a percentage of the total reads for each sample. The 'other' grouping represents summed phyla that individually contributed <1% of the total number of reads per sample; **(b)** Number of OTUs and Inverse Simpson Index. Samples at each time point are averages, median values are indicated by the solid line within each box, and the box extends to upper and lower quartile values; **(c)** Hierarchical relationships among samples based on the Yue and Clayton similarity distance matrix of 16S-OTU abundances. The hierarchical relationships between samples were obtained using the UPGMA clustering algorithm. Node labels indicate the sample/treatment; **(d)** [following page] Examples of operational taxonomic unit (OTU) changes across treatments, over time. Samples at each time point are averages of three replicates. In all figures, "T" stands for time point, control soil samples are denoted by "control", soils amended with chalcopyrite are denoted by "+ore", replicates of control soils and amended soils are indicated by "A, B or C".

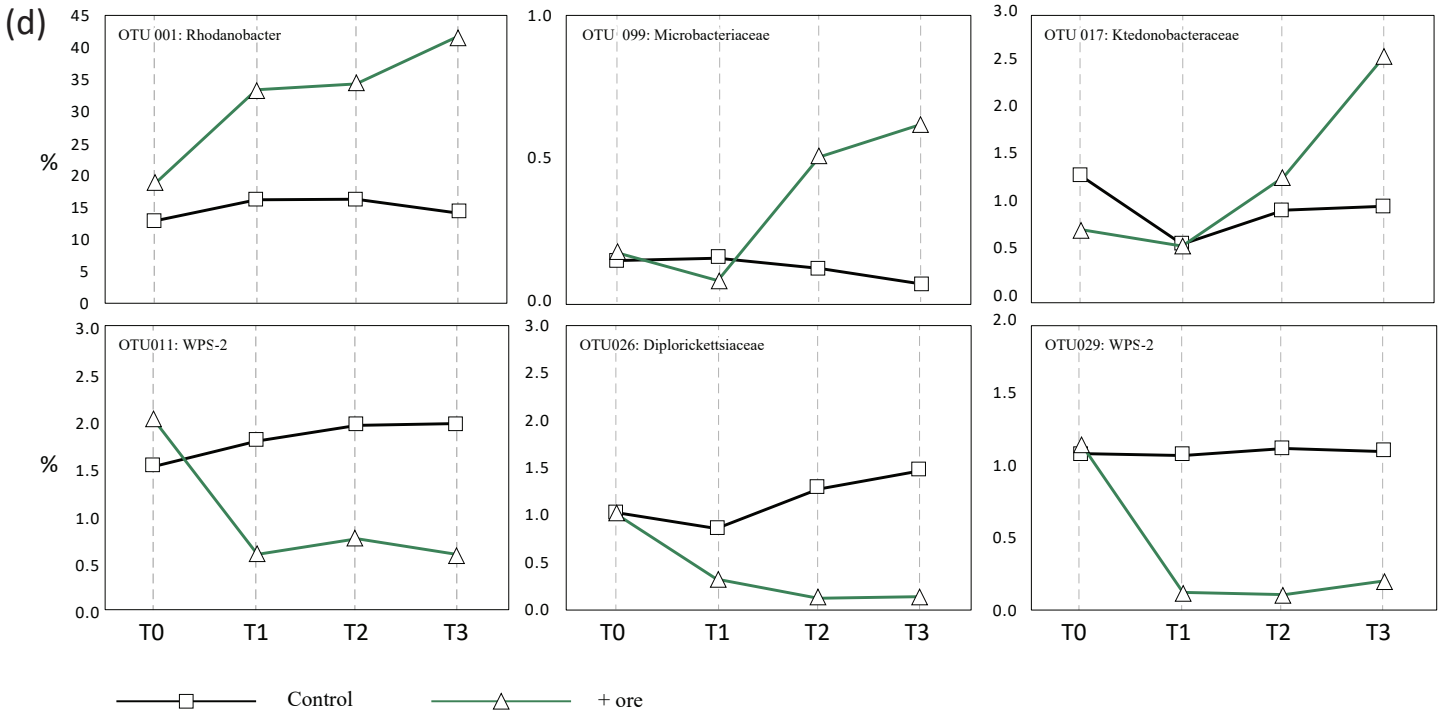

amended soils at much lower proportions (5%, 19%, 4% and 5% respectively in control soils and 2%, 11%, 1% and 1% respectively from ore amended soils). In ore amended soils, the number of OTUs at 97% sequence similarity decreased by 61%, relative to controls (on average 924 ± 51 OTUs in control samples, and on average 565 ± 67 OTUs in ore amended samples) (Figure 3b). Plots of the Inverse Simpson Index (Figure 3b), further shows that ore amendment decreases species diversity in these soils.

Relationships between ore amendment and time point (T = 0, 1, 2, 3) were evaluated through hierarchical-clustering analysis at the OTU level (Figure 3c). All control samples clustered tightly, confirming similar microbial-community compositions. Amended samples grouped apart from controls, confirming that chalcopyrite ore amendments changed the composition of the microbial community. To assess whether individual bacterial taxa were significantly different in control soils versus soils amended with ore or copper sulfate, we performed a LEfSe analysis (Segata et al. 2011) on the OTU dataset. Sample groups were set for this analysis based on their origin from "control soil" or "soils amended with ore". A number of species were significantly (P=<0.05) enriched or depleted in response to chalcopyrite ore or copper sulfate amendment, so the relative abundance of individual species normalized to the relative abundance of the same species in the controls was plotted versus time (examples shown in Figure 3d). The species that increased in response to chalcopyrite ore amendment included: Rhodanobacter sp., Ktedonobacteraceae, and Microbacteriaceae, and species that decreased in response to ore amendment included Diplorickettsiaceae, and WPS-2 unclassified species. Several of these species also responded to amendments in BC soils, and this bodes well for the use of the method with the same indicator databases across multiple soil types. The difference in "background" soil communities across sites, however, underscores the need for a database of microbial communities in Canadian soils, which would further enhance the discrimination of anomalies linked to buried mineralization from background soil communities. Sufficient data does not likely exist to create robust and representative descriptions of the taxonomic composition of BC and Canadian soils, so this work has provided a critical first step towards creating this resource. Follow on phases to this research could systematically close these knowledge gaps and create a unique resource for the province, with benefits across multiple sectors and the potential to attract sector development like new mineral deposit exploration programs facilitated by this resource.

3.2 Microbial community composition at HVC and Deerhorn

The current study's approach relies on the ability to capture microbial diversity through next-generation sequencing technologies. Analysis of these sequences reveals that the number of observed OTUs is 2671 ±445 (range 1068-3768), with an alpha diversity Chao1 index of 4066 ± 710 (range 1663–5763) and Inverse Simpson Index of 129 ± 43 (range 27-255) (Figure 4a) at HVC. The number of observed OTUs is 2418 ±344 (range 1041–3051), with an alpha diversity Chao1 index of 4016 ±814 (range 1784–5666) and Inverse Simpson Index of 85 ± 29 (range 24-169) (Figure 4b) at Deerhorn. Using the observed number of OTUs and Chao1 estimates indicates that the sequencing coverage was sufficient to capture 60% of the microbial-community

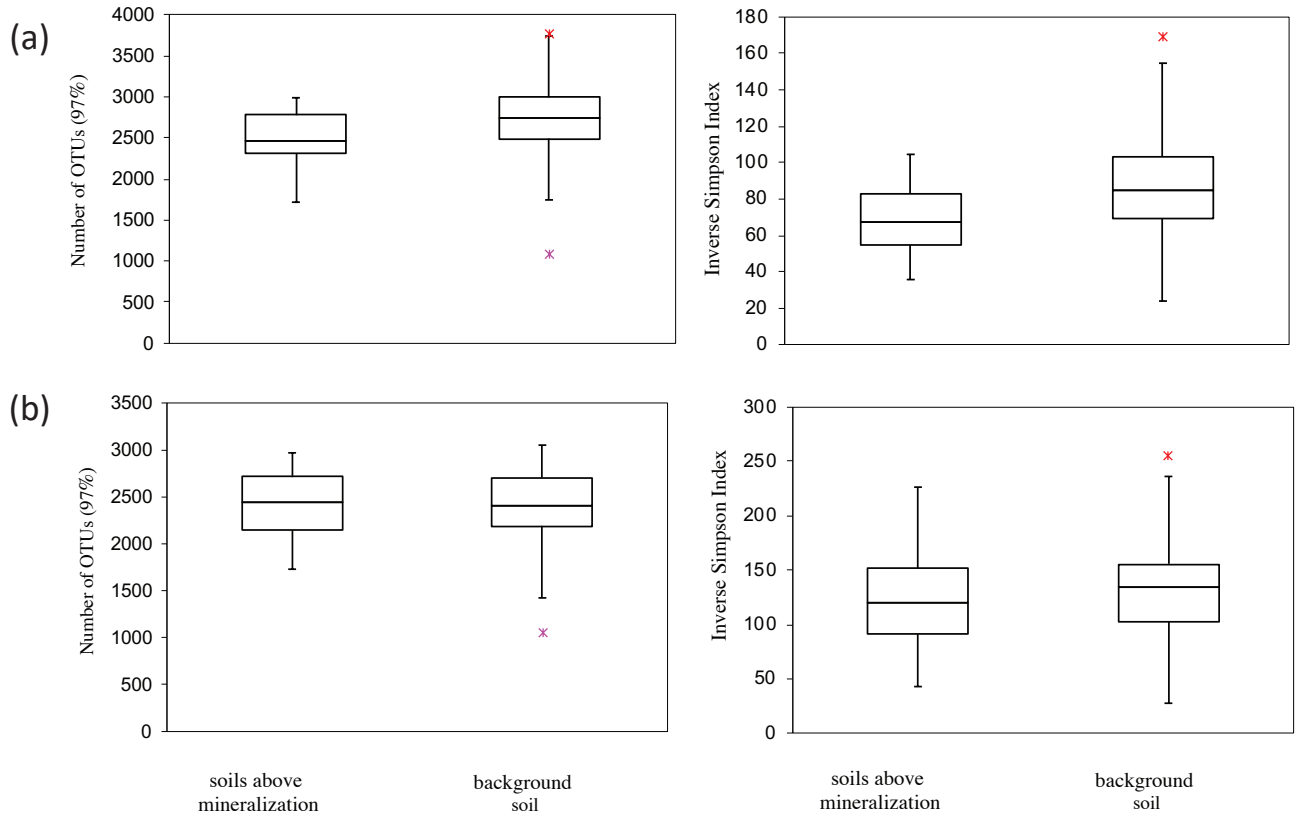

Figure 4: Number of OTUs and Inverse Simpson Index at **(a)** [preceding page] HVC; and **(b)** Deerhorn. Samples at each time point are averages, median values are indicated by the solid line within each box, and the box extends to upper and lower quartile values. Outliers are indicated by a cross. Sample groups were set for this analysis based on their origin from "background soil" or "soils above mineralization".

diversity at Deerhorn and 66% at HVC. These levels of diversity are well in line with diversity commonly observed in soils (Fierer 2017; Thompson et al. 2017). There was no pronounced difference in species richness (i.e., the number of species in a given sample) across the mineralized zone at both Deerhorn and HVC (Figure 4a, b), which is similar to the results from the incubation experiment using local soil. The number of reads per microbial phylum was normalized to total read number for a given sample and expressed as a percentage of the total reads from that sample (Figure 5a, b). Microbial community composition at HVC and Deerhorn did not vary appreciably at the phylum level between background soils and soils collected above the surface projection of mineralization. Among all the soil samples at each field site, the phyla most represented in the microbial communities belong to Proteobacteria, Acidobacteria, and Verrucomicrobia (Figure 5a, b). Lesser abundant phyla present in these communities included Actinobacteria, Bacteroidetes, Chloroflexi, Gemmatimonadetes, Planctomycetes, and unclassified bacteria at the HVC field site (Figure 5a), and Actinobacteria, Bacteroidetes, Gemmatimonadetes, Planctomycetes, Chloroflexi, Rokubacteria, and unclassified Bacteria at the Deerhorn field site (Figure 5b). The relative proportions are consistent with previous studies on soil ecosystems (Choi et al. 2017; Fierer 2017). Similar to the incubation with local soils, there were no major changes at the phyla level between soils collected across the projected surface expression of the deposit versus those collected outside this area. Unlike incubation experiments, which contained the same soil for all treatments, inter-sample variability in the field can arise due to the very high levels of microbial diversity and chemical and physical heterogeneity commonly found in soils, thus the phylum level similarity gives confidence that the analyses are not overwhelmed by this heterogeneity.

3.3 Application of microbial-community fingerprinting for deposit exploration

In traditional geochemical exploration, when surface material sampling is possible and appropriate, a suite of pathfinder elements can be used to find buried targets including Ag, As, Bi, Pb, Sb, Sn, Cu, Mo, Au, Ni, Cr, Ba, Co, Sr, Rb, Fe, K (McClenaghan and Paulen 2018), because the elements are derived from minerals that originate from the mineral deposit or associated alteration. The HVC Cu-Mo porphyry surficial soil environment is dominated by a relatively uniform till blanket, with lesser sections of waterlogged till, hummocky till, and depositional clays, with a dominant ice direction toward the southeast. When possible, the uniform till blanket was sampled as opposed to the other materials for consistency across sample media (Figure 1b).

Geochemical orientation surveys at HVC and Deerhorn show anomalous populations of different indicator and pathfinder

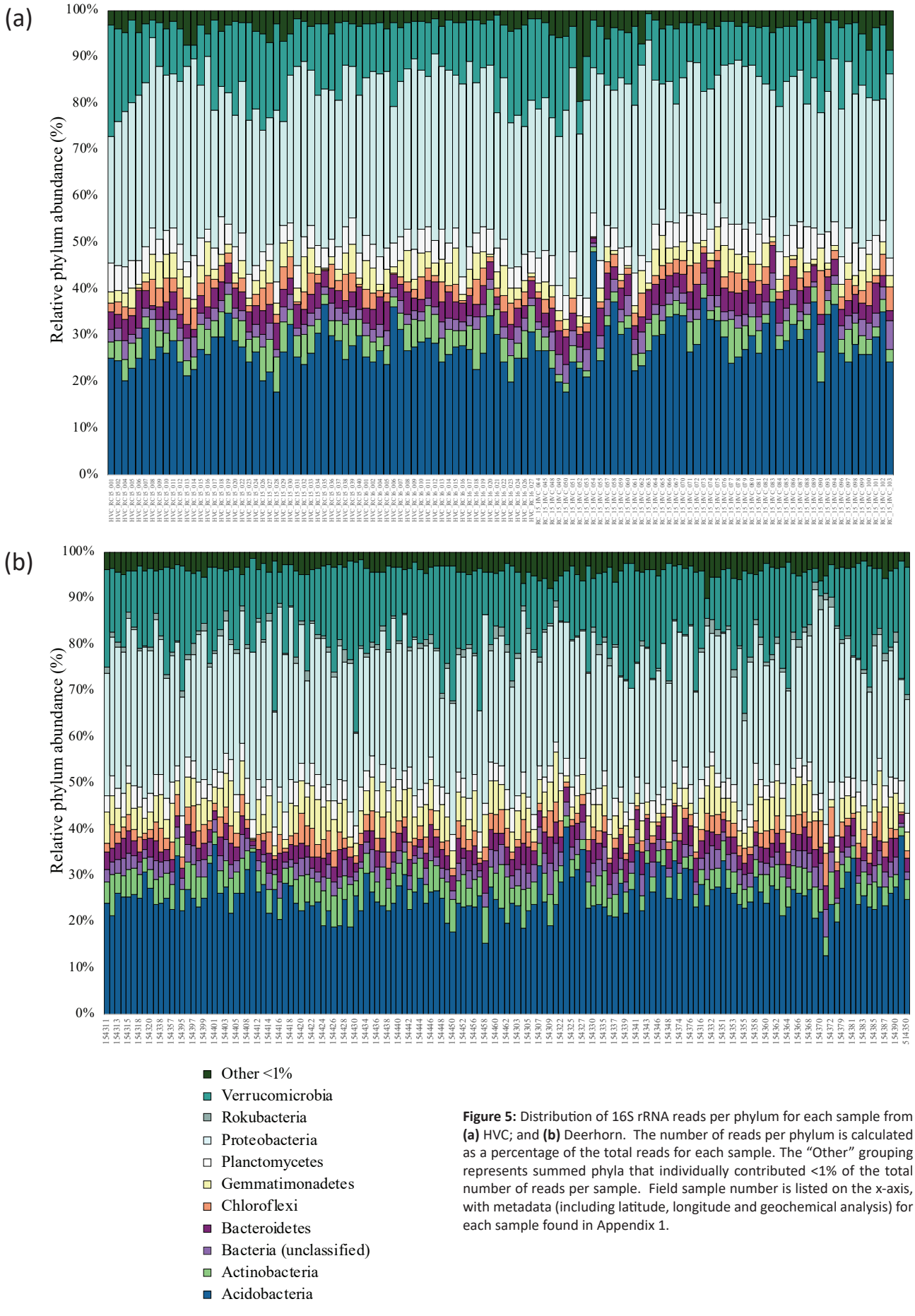

Figure 5: Distribution of 16S rRNA reads per phylum for each sample from **(a)** HVC; and **(b)** Deerhorn. The number of reads per phylum is calculated as a percentage of the total reads for each sample. The "Other" grouping represents summed phyla that individually contributed <1% of the total number of reads per sample. Field sample number is listed on the x-axis, with metadata (including latitude, longitude and geochemical analysis) for each sample found in Appendix 1.

elements in soils that can be applied to identify the buried targets, because the elements are derived from the ore and associated alteration minerals from the mineral deposit. At HVC, Cu, Mo, Ag, and Bi are best spatially correlated with the surface projection of mineralization in bedrock (0.1% Cu equivalent), seen in Figure 6a. From this suite of elements, Cu and Ag are also present in anomalous concentrations along the N-trending fault that cross-cuts bedrock mineralization. Higher concentrations of these elements above the fault are likely due to their water solubility, as they can be mobilized and travel up the structural pathway provided by the fault (for details see Chouinard, 2018). Of the pathfinder elements identified in soils at Deerhorn, the elements with anomalous populations that are most representative of the surface projection of bedrock mineralization at 0.2% Au equivalent are Cu, Mo, As, and K (Figure 6b). Indicator elements Cu and As likely originate from chalcopyrite and enargite mineralization, with Mo deriving from molybdenite, and K from the potassic alteration that is generally concentrated around zones of mineralization (for details see Rich 2016). Each of these elements for Deerhorn has been normalized to organic carbon, as

(a)

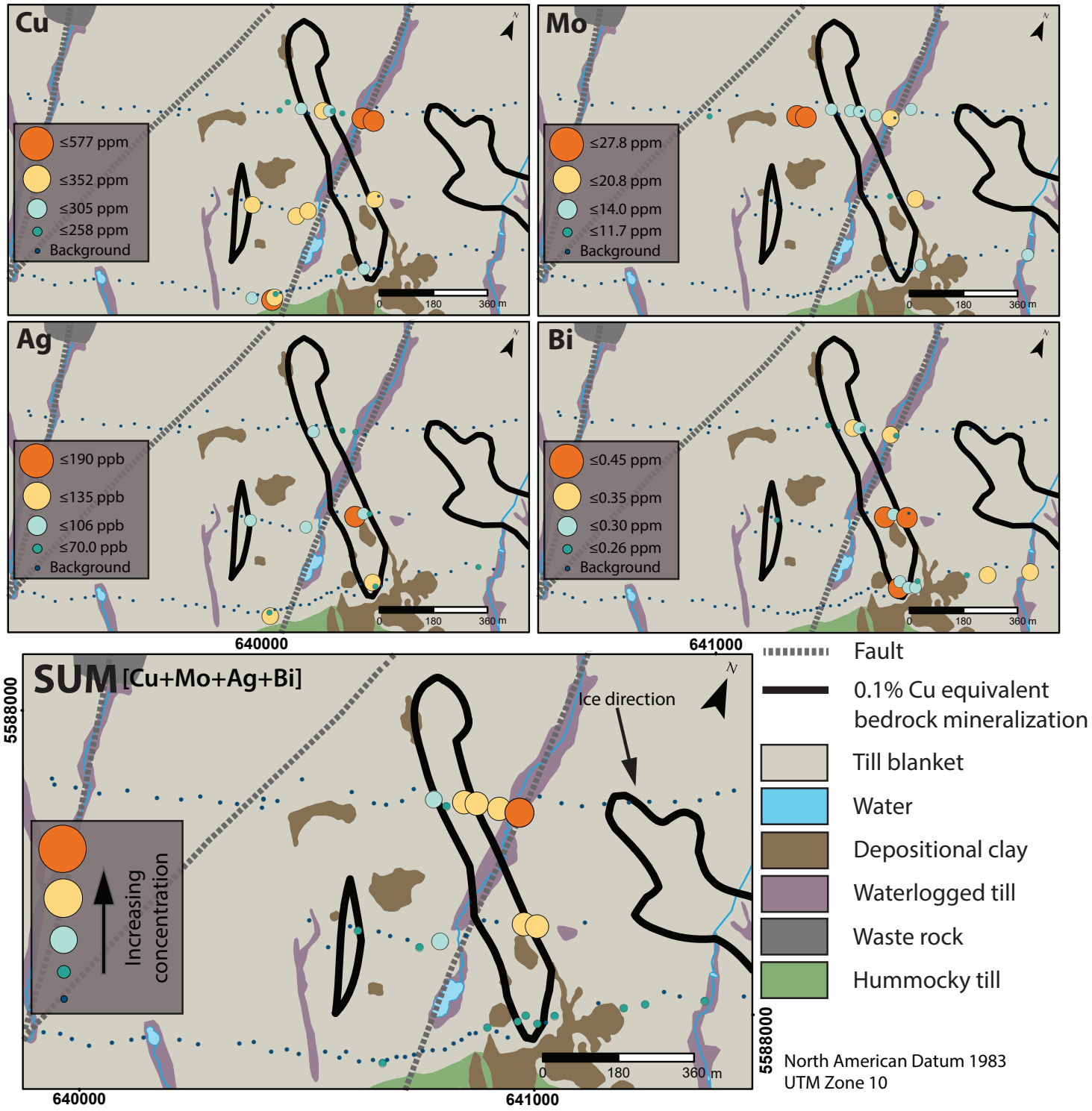

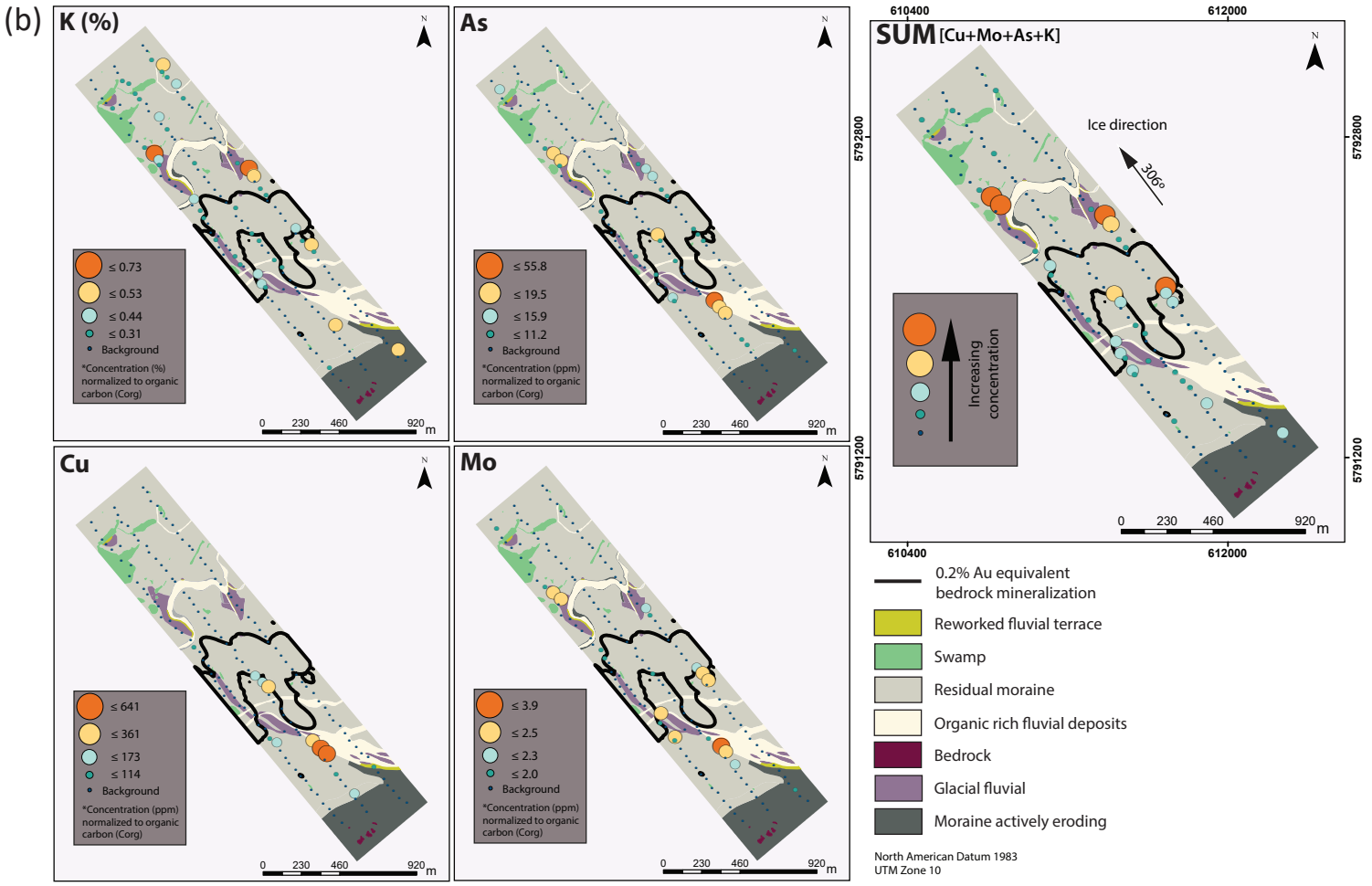

Figure 6: (a)[preceding page] Geochemical anomaly maps at HVC including Cu, Mo, Ag, Bi, and a normalized sum of these elements. Anomalies are derived from ICP-MS analysis of aqua-regia digests of soil B-horizons; **(b)** Geochemical anomaly maps at Deerhorn including K, As, Cu, Mo, and a normalized sum of these elements. Each element has been normalized to organic carbon. Anomalies are derived from ICP-MS analysis of aqua-regia digests of soil B-horizons.

the organic matter on the surface is a strong sorbent of metals and its presence in soils has the potential to skew data and produce false anomalies (Rich 2016).

Whereas the geochemical anomalies at HVC spatially resolve portions of the buried mineralization (Figure 6a), the geochemical data at Deerhorn does not accurately delineate the porphyry through cover. The anomalous signals in indicator and pathfinder chemistry at Deerhorn have not been well developed and do not have a strong spatial correlation with ore mineralization (Figure 6b). The discrepancies in the outcomes of geochemical deposit-scale exploration between the two field sites supports the conclusion that even though geochemical tools work well in some environments, other areas that are host to potentially economic deposits may be missed using these methods due to false negatives—particularly when there has been complicated evolution of the surficial landscape with multiple generations of ice flow and deposition, and where overburden is especially thick (>25 m). The geochemical data at HVC show anomalies that spatially correspond to subsurface mineralization (Figure 6a), but where till is thicker at Deerhorn with different ice-flow directions, we do not see full resolution of the mineral target (Figure 6b). Geochemical signals may be transported and may not always develop in the surface environment as evidenced by the Deerhorn porphyry deposit. A geomicrobiological approach to mineral exploration aims to more robustly identify porphyry deposits in covered terrain, as the soil microbial community is likely sensitive to chemical variability in soils that is less than what is resolvable with current methods of chemical analysis.

To assess whether individual bacterial taxa were significantly different in soils above the surface expression of porphyry mineralization versus background, we performed a LEfSe analysis (Segata et al. 2011) on the OTU dataset. Sample groups were set for this analysis based on their origin from “background soil” or “soils above mineralization”. Soils above mineralization are defined based on the surface projection of mineralization: 0.1% Cu equivalent for HVC and 0.2% Au equivalent for Deerhorn. From the indicator species (OTUs) that were generated from the LefSe, species showing best spatial correlation with mineralization were charted onto deposit-scale exploration maps in a fashion analogous to mapping of geochemical anomalies (Fig-

ure 7 and 8). From the LEfSe analysis, we produced two types of indicators; positive (higher relative abundance of bacterial taxa above the deposit surface expression than background) and negative (lower relative abundance of bacterial taxa above the deposit surface expression than background).

Our analyses show significant (p-value for all OTUs <0.05) differences in species' relative abundance in response to ore mineralization. For HVC, there are 24 indicators with 9 positive indicator species and 15 negative indicator species. The majority of the positive indicator species are assigned to the phylum Acidobacteria and the negative indicator species primarily belong to phyla Proteobacteria and Acidobacteria. At Deerhorn, the analysis provided 47 indicators with 32 positive indicator species and 15 negative indicator species. Proteobacteria and Acidobacteria are the dominant phyla represented by the positive indicator species and the negative indicator species are assigned to Verrucomicrobia and Proteobacteria. Each of these indicator species represent a unique microbial sensor that is indicative of potential porphyry-style mineralization. Differences in relative abundance of microbial indicator species can be used to spatially resolve subsurface mineralization at HVC and Deerhorn porphyry deposits. Indicator species show both enrichment and depletion correlated with the spatial extent of subsurface mineralization at both field sites (Figure 7a,b; Figure 8a). At each deposit, the geochemical gradients in the surficial soil environment as a function of the buried of mineralization are reflected by spatial variability in the microbial communities. These targets have been resolved by indicator species in covered terrain with till thickness ranging from <10 m to 60 m. Establishing indicator species from areas where the location of mineralization is known is useful for developing a fingerprint for porphyry-type indicators; however, for the purposes of potential microbial-based mineral exploration, site to site reproducibility with shared indicators is necessary.

A suite of indicator species that are shared between both field sites and lab incubations can also resolve buried mineralization; however, species enriched above mineralization exhibit more accurate spatial resolution than negative indicator species. A total of 52 positive indicator species and 28 negative indicator species make up our current porphyry fingerprint. Positive and negative indicator species are mainly comprised of Proteobacteria and Acidobacteria with some species belonging to Verrucomicrobia, similar to the deposit specific fingerprints. Species belonging to the phylum Chloroflexi exclusively show enrichments above the porphyries as well, which is comparable to the increased relative abundance in this phylum in both copper incubation experiments. Whereas increases in relative abundances of Chloroflexi have been shown in the literature to increase in copper-rich soil environments (Chodak et al. 2016; Yin et al. 2015), other studies report decreases in relative abundances with higher concentrations of copper (Chen et al. 2018; Li et al. 2015; Tipayno et al. 2018). Therefore, an enrichment of species in this phylum cannot conclusively be linked to buried copper mineralization. Examples of the positive and negative indicator species from the combined fingerprint are shown in Figure 7c and Figure 8b. Positive indicator species display better spatial distribution with HVC and Deerhorn mineralization relative to the negative indicator species. This discrepancy in the quality of the different types of microbial indicators above porphyries could be due to the large spatial expanse of porphyry mineralization and alteration. Surficial geochemistry exploration surveys depend upon the sampling of background soils that do not contain anomalous signatures, and in the case of these studies, we have likely not sampled beyond the farthest extent of the porphyry footprint. The nature of porphyry mineralization distribution is gradational, thus there is potential that indicator species are responding to these diffuse boundaries, leading to a weaker anomaly. Despite these issues, indicator species are resolving the concealed porphyry deposits with changes in relative abundance occurring directly over surface projections of mineralization, and the set of indicator species is conserved across experimental data and two separate copper porphyry deposits.

4. CONCLUSION

This research has determined that using microbiome fingerprinting with high-throughput sequencing technologies to explore for buried porphyry mineralization is feasible, offering more potential indicators than traditional geochemistry. Of those potential indicators, a greater percentage effectively resolves the buried porphyries at HVC and Deerhorn. Given that a single soil sample may host thousands of microbial taxa, each containing hundreds to thousands of genes, the potential microbial indicators greatly outweigh the fixed number of elements used during geochemical anomaly detection, demonstrating the statistical power of this approach to identifying deposits through cover. The integration of microbial community information with soil chemistry and landscape development, coupled with geology and geophysics significantly improves the decision-making process when drilling potential deposits, as target delineation becomes more accurate. In so doing, sequence-based exploration could go a long way towards helping the resource sector meet future demand and support the growing needs of the technology sector. At the same time, the finding that information stored in the DNA of soil microbes can be used as a fingerprint of underlying geological features suggest much broader application of DNA-based sequencing approaches to trace subtle anomalies and variability in natural and engineered environments. Our ability to harness sequence information from the environment will continue to enhance our interaction with the Earth system and support the growing global bioeconomy.

(a)

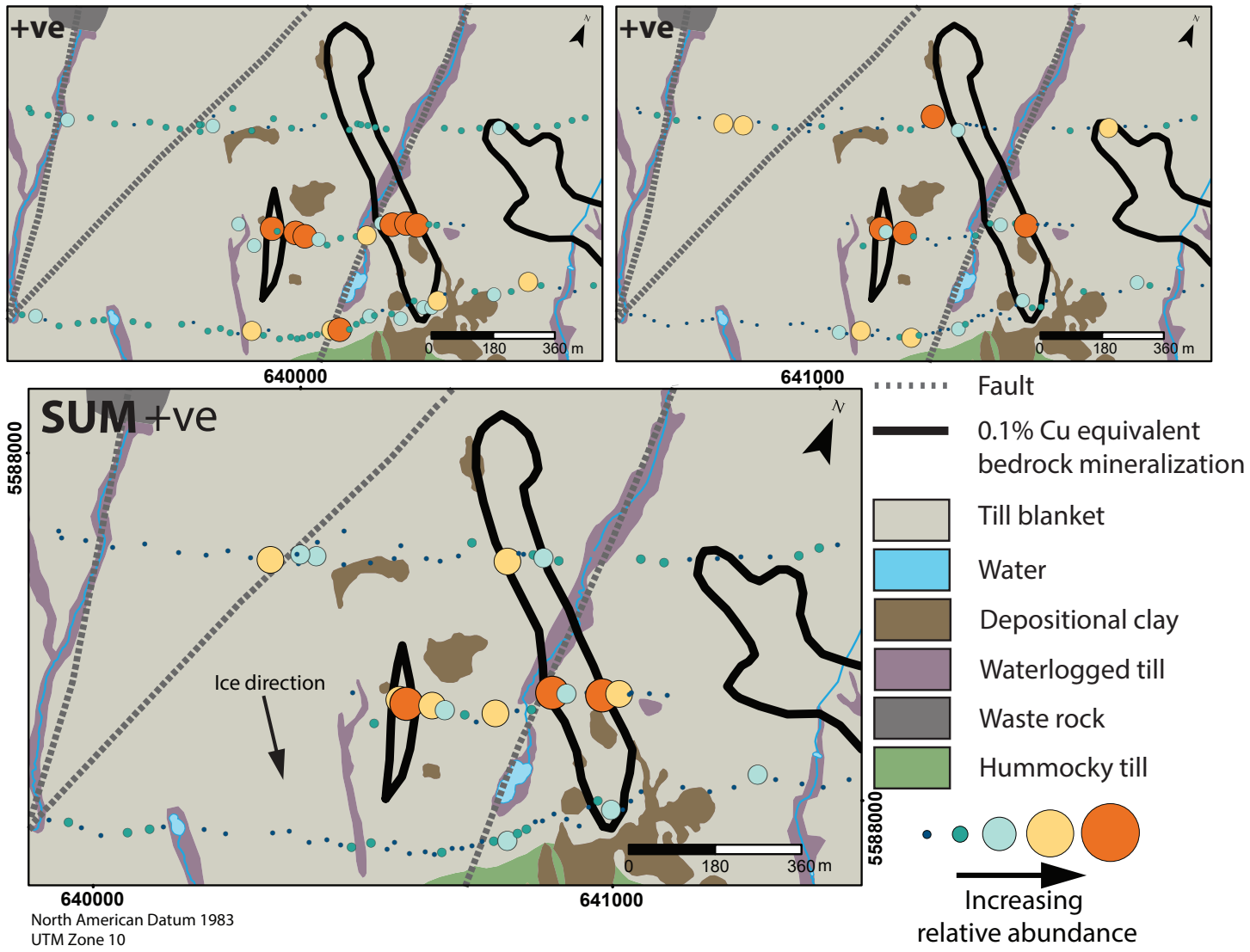

5. ACKNOWLEDGMENTS

Previous students of the MDRU–Mineral Deposit Research Unit's Exploration Geochemistry Initiative (EGI) are credited for their sampling efforts, surficial mapping, and processing of geochemical data: Rachel Chouinard - Highland Valley Copper, Highmont South Cu-Mo Porphyry Deposit; and Shane Rich - Woodjam Deerhorn Cu-Au Porphyry Deposit. The authors thank S. Rich and R. Chouinard for sample collection. The Teck Resources Limited personnel at Highland Valley Copper are greatly appreciated for allowing access to the site and guidance in the field. Consolidated Woodjam Copper are also thanked for site access. Funding was generously provided by Geoscience BC. B.P. Iulianella Phillips was also the recipient of a 2018 Geoscience BC Student Scholarship.

6. REFERENCES

Anderson, R., Plouffe, A., Ferbey, T. and C. Dunn (2012). The search for surficial expressions of buried Cordilleran porphyry deposits: background and progress in a new Targeted Geoscience Initiative 4 activity in the southern Canadian Cordillera, British Columbia; Geological Survey of Canada, Current Research (online) 2012-7. doi:10.4095/290295

Apprill, A., S. McNally, R. Parsons and L. Weber (2015). "Minor revision to V4 region SSU rRNA 806R gene primer greatly increases detection of SAR11 bacterioplankton." Aquatic Microbial Ecology 75(2): 129-137. doi: https://doi.org/10.3354/ame01753

Binladen, J., M. T. P. Gilbert, J. P. Bollback, F. Panitz, C. Bendixen, R. Nielsen and E. Willerslev (2007). "The use of coded PCR prim-

(b)

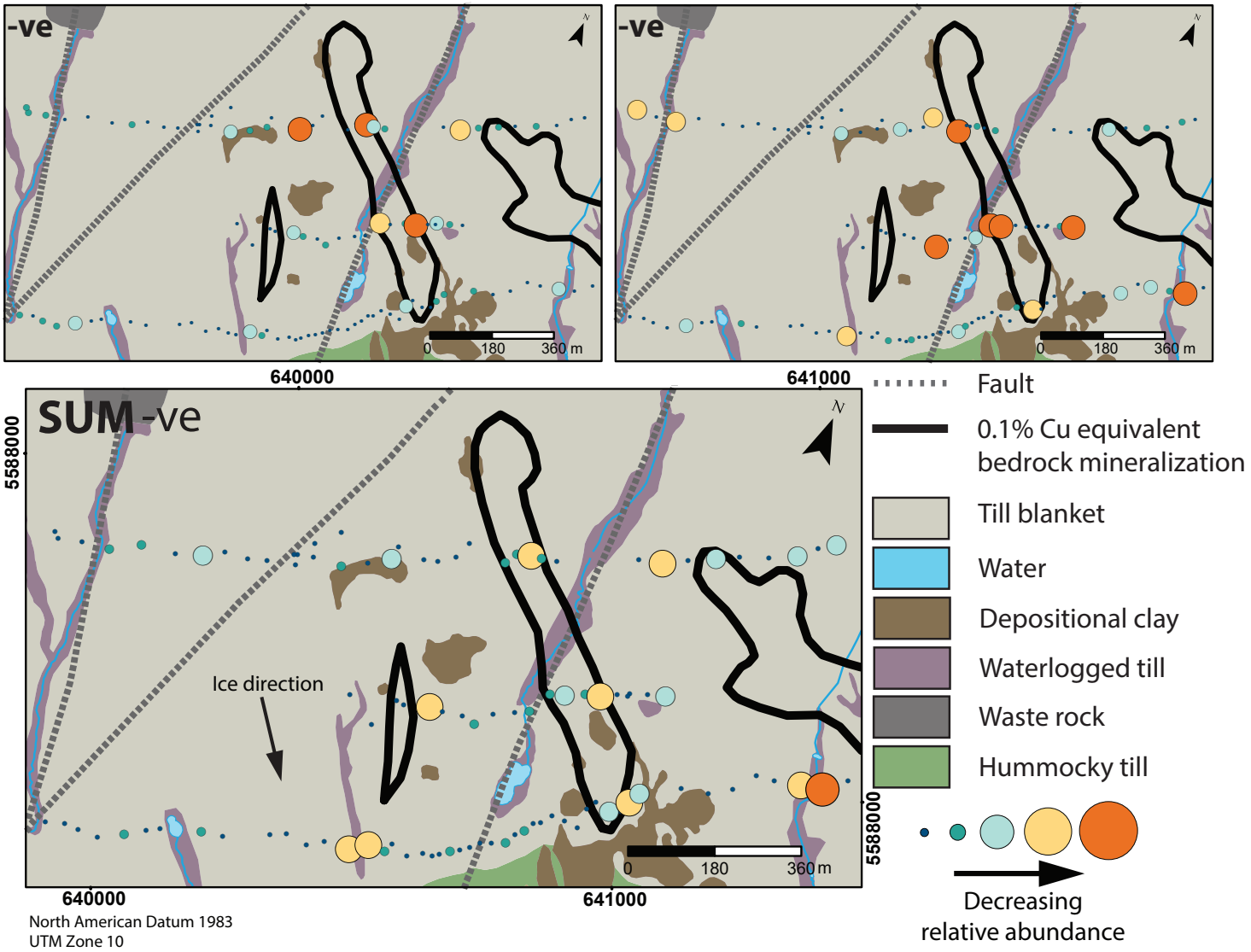

Figure 7: (a) [preceding page] HVC deposit-scale anomaly maps of the enriched (positive (+ve)) indicator species that show an increase in relative abundance above bedrock mineralization (0.1% Cu equivalent). These indicator species are predicted from a LefSe indicator species analysis whereby species that show significant (p-value <0.05) differences between soils above subsurface mineralization and those from the background soils are identified. A normalized sum for these positive indicator species is also charted onto a deposit map; **(b)** HVC deposit-scale anomaly maps of the depleted (negative (-ve)) indicator species that show a decrease in relative abundance above bedrock mineralization (0.1% Cu equivalent). These indicator species are predicted from a LefSe indicator species analysis whereby species that show significant (p-value <0.05) differences between soils above subsurface mineralization and those from the background soils are identified. A normalized sum for these negative indicator species is also charted onto a deposit map; **(c) [following page]**Normalized sums for the enriched (positive (+ve)) indicator species and depleted (negative (-ve)) indicator species are plotted as deposit-scale anomaly maps at HVC. These sums are a combination of indicator species predicted from a LefSe analysis that are shared between HVC, Deerhorn, and copper incubation experiments.

(c)

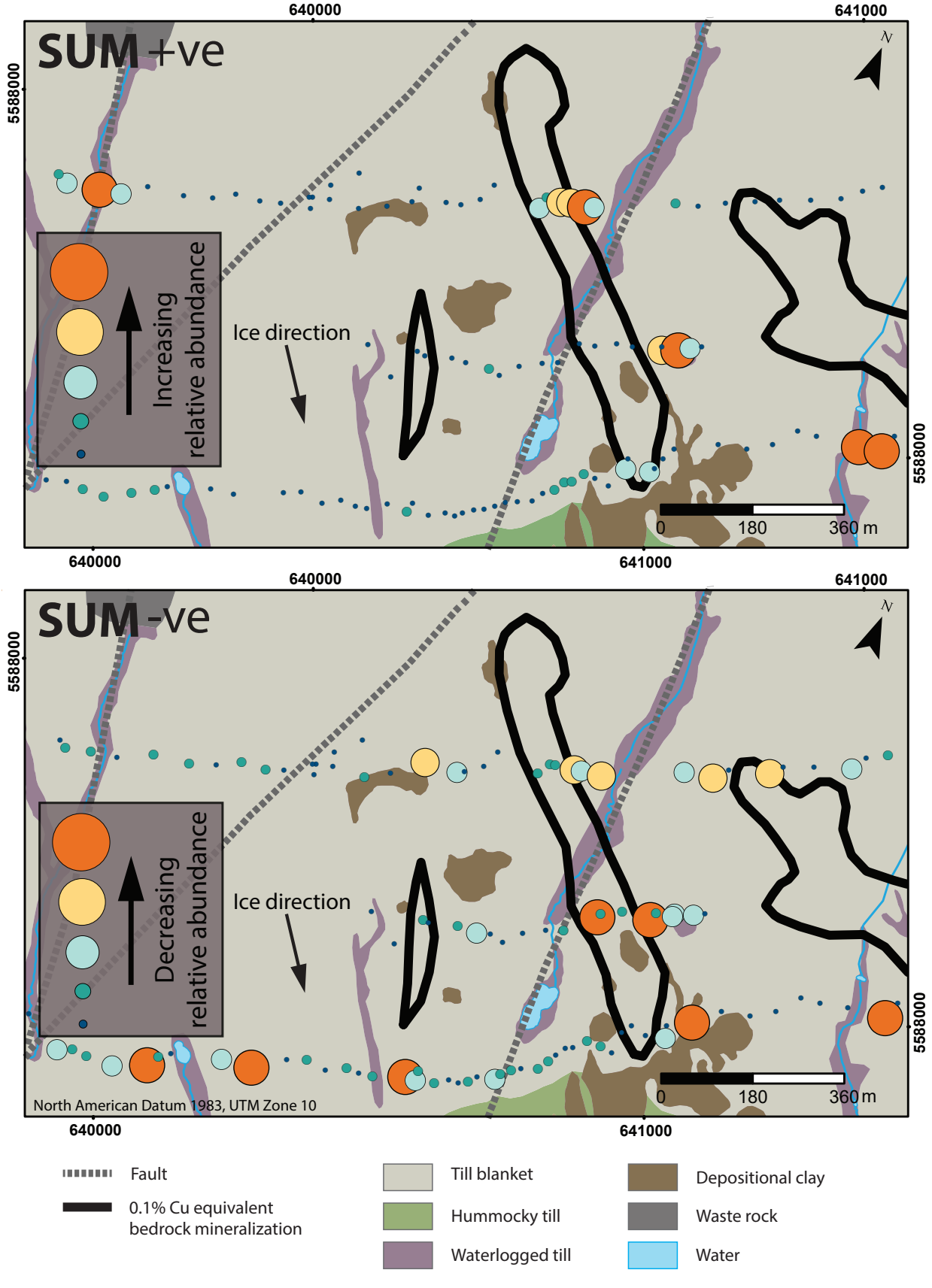
SUM +ve
640000
641000
5588000
Increasing relative abundance
Ice direction
0
180
360 m
SUM -ve
Decreasing relative abundance
North American Datum 1983, UTM Zone 10
Fault
0.1% Cu equivalent bedrock mineralization
Till blanket
Hummocky till
Waterlogged till
Depositional clay
Waste rock
Water

(a)

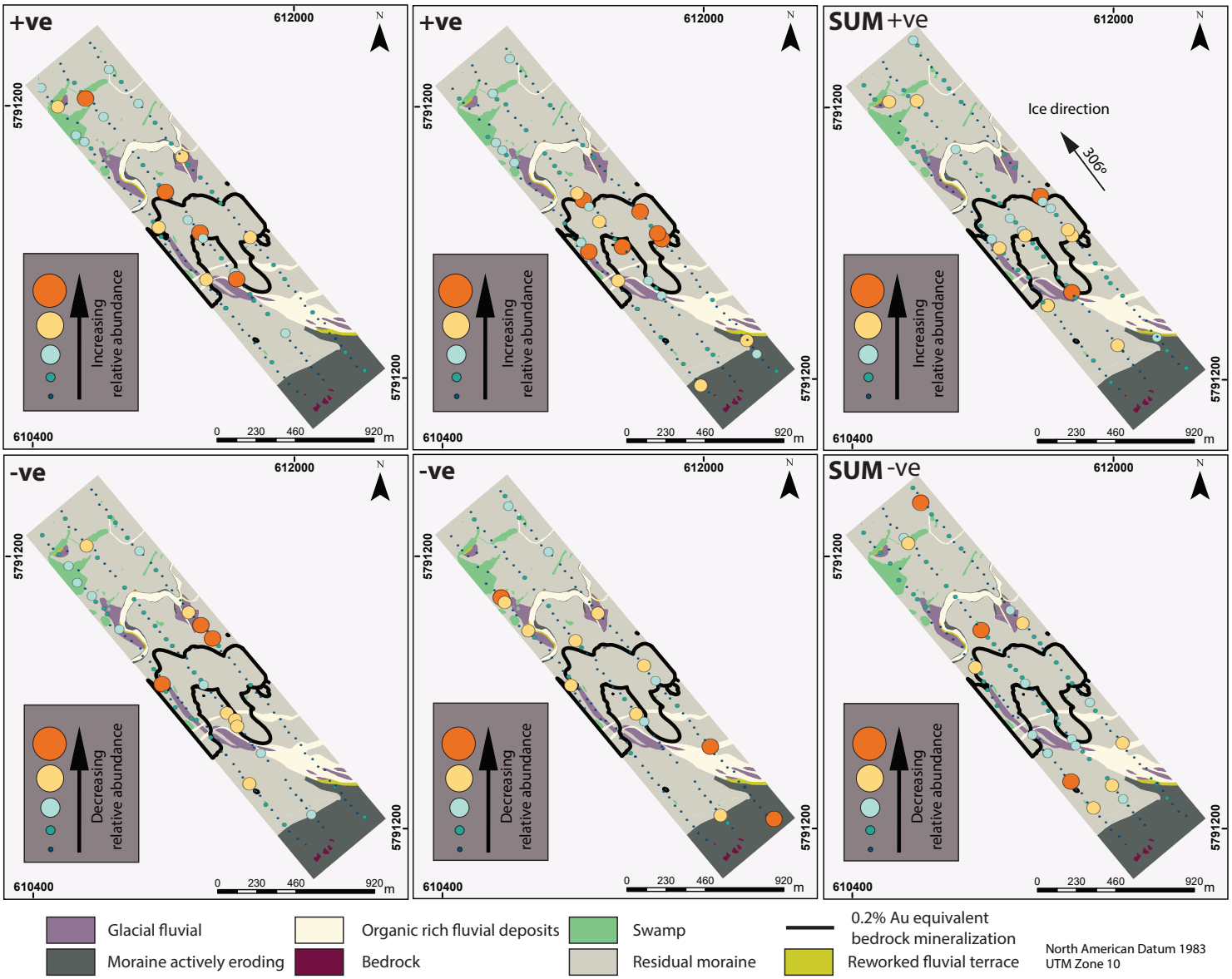

Figure 8: (a) Deerhorn deposit-scale anomaly maps at of the enriched (positive (+ve)) indicator species that show an increase in relative abundance above subsurface bedrock mineralization (0.2% Au equivalent) and the depleted (negative (-ve)) indicator species that show a decrease in relative abundance above mineralization (0.2% Au equivalent). These indicator species are predicted from a LefSe indicator species analysis whereby species that show significant (p-value <0.05) differences between soils above subsurface mineralization and those from the background soils are identified. A normalized sum for both enriched (positive (+ve)) and depleted indicator species (negative(-ve)) is also charted onto a deposit map; **(b)** Normalized sums for the enriched (positive (+ve)) indicator species and depleted (negative (-ve)) indicator species are plotted as deposit-scale anomaly maps at Deerhorn. These sums are a combination of indicator species predicted from a LefSe analysis that are shared between HVC, Deerhorn, and copper incubation experiments.

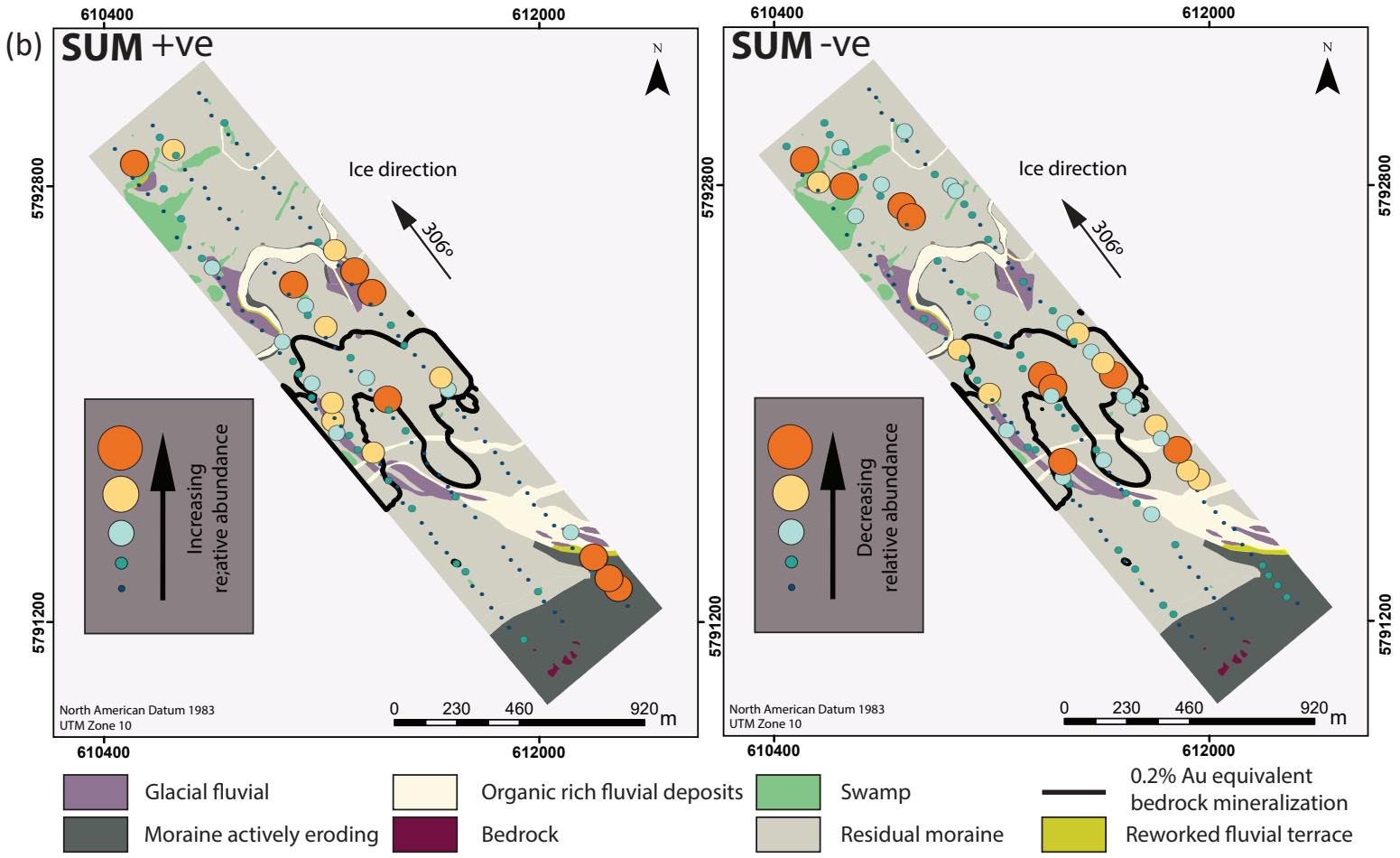

ers enables high-throughput sequencing of multiple homolog amplification products by 454 parallel sequencing." PloS one 2(2): e197. doi: 10.1371/journal.pone.0000197

Bissig, T. and R. Riquelme (2010). "Andean uplift and climate evolution in the southern Atacama Desert deduced from geomorphology and supergene alunite-group minerals." Earth and Planetary Science Letters 299(3): 447-457. doi: 10.1016/j.epsl.2010.09.028

Cameron, E. M., S. M. Hamilton, M. I. Leybourne, G. E. Hall and M. B. McClenaghan (2004). "Finding deeply buried deposits using geochemistry." Geochemistry: Exploration, Environment, Analysis 4(1): 7-32. doi: 10.1144/1467-7873/03-019

Caporaso, J. G., C. L. Lauber, W. A. Walters, D. Berg-Lyons, C. A. Lozupone, P. J. Turnbaugh, N. Fierer and R. Knight (2011). "Global patterns of 16S rRNA diversity at a depth of millions of sequences per sample." Proceedings of the National Academy of Sciences 108(Supplement 1): 4516-4522. doi: /10.1073/pnas.1000080107

Chen, Y., Jiang, Y., Huang, H., Mou, L., Ru, J., Zhao, J., and Xiao, S. (2018). "Long-term and high-concentration heavy-metal contamination strongly influences the microbiome and functional genes in Yellow River sediments." Science of the Total Environment 637:1400–1412. doi: 10.1016/j.scitotenv.2018.05.109

Chodak, M., Klimek, B., and M. Nikli´nska (2016). "Composition and activity of soil microbial communities in different types of temperate forests." Biology and Fertility of Soils 1093:1093–1104. doi: 10.1007/s00374-016-1144-2

Choi, J., F. Yang, R. Stepanauskas, E. Cardenas, A. Garoutte, R. Williams, J. Flater, J. M. Tiedje, K. S. Hofmockel and B. Gelder (2017). "Strategies to improve reference databases for soil microbiomes." The ISME journal 11(4): 829. doi:10.1038/ismej.2016.168

Chao, A. 1984. "Non-parametric estimation of the number of classes in a population." Scandinavian Journal of Statistics 11:265-270. doi: 10.2307/4615964

Chouinard, R.L., Winterburn, P.A., Ross, M. and R.G. Lee (2017): Surficial geochemical footprint of buried porphyry Cu-Mo mineralization at the Highland Valley Copper operations, south-central British Columbia: project update; In: Geoscience BC Summary of Activities 2016, Geoscience BC, Report 2017-1, p. 125–132.

Chouinard, R. L. (2018). Surficial geochemical tools for Cu-Mo porphyry exploration in till-covered terrain. MSc Thesis, The University of British Columbia.

Edgar, R. C., B. J. Haas, J. C. Clemente, C. Quince and R. Knight (2011). "UCHIME improves sensitivity and speed of chimera

detection." Bioinformatics 27(16): 2194-2200. doi: 10.1093/bioinformatics/btr381.

Falkowski, P. G., T. Fenchel and E. F. Delong (2008). "The microbial engines that drive Earth's biogeochemical cycles." Science 320(5879): 1034-1039. doi: 10.1126/science.1153213

Ferbey, T., Anderson, R.G. and A. Plouffe (2014): An integrated approach to search for buried porphyry-style mineralization in central British Columbia using geochemistry and mineralogy: a TGI-4 project; Geological Survey of Canada, Current Research (online) 2014-2, 15 p. doi:10.4095/293130

Fierer, N. (2017). "Embracing the unknown: disentangling the complexities of the soil microbiome." Nature Reviews Microbiology 15(10): 579-590. Doi:10.1038/nrmicro.2017.87

Gavrilov, S. N., A. A. Korzhenkov, I. V. Kublanov, R. Bargiela, L. Zamana, A. Popova, S. Toshchakov, P. Golyshin and O. V. Golyshina (2019). "Microbial communities of polymetallic deposits' acidic ecosystems of continental climatic zone with high temperature contrasts." Frontiers in microbiology 10: 1573. doi: 10.3389/fmicb.2019.01573

Gilliss, M., T. Al, D. Blowes, G. Hall and B. MacLean (2004). "Geochemical dispersion in groundwater from a weathered Cu–Zn deposit in glaciated terrain." Geochemistry: Exploration, Environment, Analysis 4(4): 291-305. doi: 10.1144/1467-7873/04-206

Hallberg, K. B., K. Coupland, S. Kimura and D. B. Johnson (2006). "Macroscopic streamer growths in acidic, metal-rich mine waters in North Wales consist of novel and remarkably simple bacterial communities." Applied and environmental microbiology 72(3): 2022-2030. doi: 10.1128/AEM.72.3.2022-2030.2006

Hamilton, S. (1998). "Electrochemical mass-transport in overburden: a new model to account for the formation of selective leach geochemical anomalies in glacial terrain." Journal of Geochemical Exploration 63(3): 155-172. doi: 10.1016/S0375-6742(98)00052-1

Heberlein, D. R. and H. Samson (2010). "An assessment of soil geochemical methods for detecting copper-gold porphyry mineralization through Quaternary glaciofluvial sediments at the Kwanika Central Zone, north-central British Columbia." Geoscience BC Report 2010-03.

Hughes, J. B., J. J. Hellmann, T. H. Ricketts and B. J. Bohannan (2001). "Counting the uncountable: statistical approaches to estimating microbial diversity." Applications in Environmental Microbiology 67(10): 4399-4406. doi: 10.1128/AEM.67.10.4399-4406.2001

Kaiser, K., B. Wemheuer, V. Korolkow, F. Wemheuer, H. Nacke, I. Schöning, M. Schrumpf and R. Daniel (2016). "Driving forces of soil bacterial community structure, diversity, and function in temperate grasslands and forests." Scientific Reports 6: 33696. doi: 10.1038/srep33696

Kelley, D. L., K. D. Kelley, W. B. Coker, B. Caughlin and M. E. Doherty (2006). "Beyond the obvious limits of ore deposits: The use of mineralogical, geochemical, and biological features for the remote detection of mineralization." Economic Geology 101(4): 729-752. doi: 10.2113/gsecongeo.101.4.729

Kesler, S. E. (2007). Mineral supply and demand into the 21st century. Proceedings for a Workshop on Deposit Modeling, Mineral Resource Assessment, and Their Role in Sustainable Development. U.S. Geological Survey circular (Vol. 1294, pp. 55-62).

Koh, H.-W., H. Hong, U.-G. Min, M.-S. Kang, S.-G. Kim, J.-G. Na, S.-K. Rhee and S.-J. Park (2015). "Rhodanobacter aciditrophus sp. nov., an acidophilic bacterium isolated from mine wastewater." International Journal of Systematic and Evolutionary Microbiology 65(12): 4574-4579. doi: 10.1099/ijsem.0.000614

Li, J., Ma, Y. B., Hu, H. W., Wang, J. T., Liu, Y. R., and J.Z. He (2015). "Field-based evidence for consistent responses of bacterial communities to copper contamination in two contrasting agricultural soils." Frontiers in Microbiology, 6(31). doi: 10.3389/fmicb.2015.00031

Lusty, P.A.J. and A.G. Gunn (2015). "Challenges to global mineral resource security and options for future supply." Geological Society, London, Special Publications 393(1): 265-276. doi: 10.1144/SP393.13

Magurran, A. E. (2013). Measuring Biological Diversity, John Wiley & Sons.

McClenaghan, M. and R. Paulen (2018). "Application of till mineralogy and geochemistry to mineral exploration." In: Past Glacial Environments, Elsevier: pp 689-751. doi: 10.1016/B978-0-08-100524-8.00022-1

Newman, D. K. and J. F. Banfield (2002). "Geomicrobiology: How molecular-scale interactions underpin biogeochemical systems." Science 296(5570): 1071-1077. doi: 10.1126/science.1010716

Nordstrom, D. K. (2011). "Hydrogeochemical processes governing the origin, transport and fate of major and trace elements from mine wastes and mineralized rock to surface waters." Applied Geochemistry 26(11): 1777-1791. doi: 10.1016/j.apgeochem.2011.06.002

Plouffe, A., T. Ferbey, R. Anderson, S. Hashmi and B. Ward (2013a). "New TGI-4 till geochemistry and mineralogy results near the Highland Valley, Gibraltar, and Mount Polley mines, and Woodjam District: An aid to search for buried porphyry deposits." Geological Survey of Canada Open File 7473: 58.

Plouffe, A., T. Ferbey, R. Anderson, S. Hashmi, B. Ward and D. Sacco (2013b). "The use of till geochemistry and mineralogy to explore for buried porphyry deposits in the Cordillera—prelimi-

nary results from a TGI-4 intrusion-related ore systems project." Geological Survey of Canada Open File 7367, poster.

Reid, N., S. Hill and D. Lewis (2009). "Biogeochemical expression of buried gold mineralization in semi-arid northern Australia: penetration of transported cover at the Titania Gold Prospect, Tanami Desert, Australia." Geochemistry: Exploration, Environment, Analysis 9(3): 267-273. doi.org/10.1144/1467-7873/09-194

Rich, S.D. and P.A. Winterburn (2016): Geochemical mapping of the Deerhorn copper-gold porphyry deposit and associated alteration through transported cover, central British Columbia (NTS 093A/03). In: Geoscience BC Summary of Activities 2015, Geoscience BC, Report 2016-1, p. 167–174.

Rich, S. (2016). Geochemical mapping of porphyry deposits and associated alteration through transported overburden. MSc Thesis, The University of British Columbia.

Roesch, L. F., R. R. Fulthorpe, A. Riva, G. Casella, A. K. Hadwin, A. D. Kent, S. H. Daroub, F. A. Camargo, W. G. Farmerie and E. W. Triplett (2007). "Pyrosequencing enumerates and contrasts soil microbial diversity." The ISME journal 1(4): 283. doi: 10.1038/ismej.2007.53

Schloss, P. D., D. Gevers and S. L. Westcott (2011). "Reducing the effects of PCR amplification and sequencing artifacts on 16S rRNA-based studies." PloS one 6(12): e27310. doi:10.1371/journal.pone.0027310

Schloss, P. D., S. L. Westcott, T. Ryabin, J. R. Hall, M. Hartmann, E. B. Hollister, R. A. Lesniewski, B. B. Oakley, D. H. Parks and C. J. Robinson (2009). "Introducing mothur: open-source, platform-independent, community-supported software for describing and comparing microbial communities." Applied and Environmental Microbiology 75(23): 7537-7541. doi: 10.1128/AEM.01541-09

Segata, N., J. Izard, L. Waldron, D. Gevers, L. Miropolsky, W. S. Garrett and C. Huttenhower (2011). "Metagenomic biomarker discovery and explanation." Genome Biology 12(6): R60. doi: 10.1186/gb-2011-12-6-r60

Singer, V. L., L. J. Jones, S. T. Yue and R. P. Haugland (1997). "Characterization of PicoGreen reagent and development of a fluorescence-based solution assay for double-stranded DNA quantitation." Analytical Biochemistry 249(2): 228-238. doi: 10.1006/abio.1997.2177

Stackebrandt, E. (2014). "The Family Acidimicrobiaceae" In: The Prokaryotes, Springer: Berlin, Heidelberg, Germany pp 5-12. doi: 10.1007/978-3-642-30138-4_198

Stanley, C. (2003). "Statistical evaluation of anomaly recognition performance." Geochemistry: Exploration, Environment, Analysis 3(1): 3-12. doi: 10.1144/1467-787302-040

Thompson, L. R., J. G. Sanders, D. McDonald, A. Amir, J. Ladau, K. J. Locey, R. J. Prill, A. Tripathi, S. M. Gibbons and G. Ackermann (2017). «A communal catalogue reveals Earth's multiscale microbial diversity.» Nature 551(7681): 457. doi: 10.1038/nature24621

Tipayno, S. C., Truu, J., Samaddar, S., Truu, M., Preem, J.-K., Oopkaup, K., Espenberg, M., Chatterjee, P., Kang, Y., Kim, K., and T. Sa (2018). "The bacterial community structure and functional profile in the heavy metal contaminated paddy soils, surrounding a nonferrous smelter in South Korea." Ecology and Evolution 8:6157–6168. doi: 10.1002/ece3.4170

Torsvik, V. and L. Øvreås (2002). "Microbial diversity and function in soil: from genes to ecosystems." Current opinion in microbiology 5(3): 240-245. doi: 10.1016/S1369-5274(02)00324-7

Townley, B., A. Puig, G. Ojeda, R. Luca, T. Vargas, J. Leroux and B. Milkereit (2007). Understanding real time processes behind the development of surface geochemical expressions from ore bodies beneath cover: Source to surface and detection by means of collector devices. In: Proceedings of Exploration, vol. 7, pp. 1019-1021.

Westcott, S. L. and P. D. Schloss (2017). "OptiClust, an improved method for assigning amplicon-based sequence data to operational taxonomic units." mSphere 2(2): e00073-00017. doi: 10.1128/mSphereDirect.00073-17

Wickham A, Winterburn, P. A., and B. Elliott. (2019). "Till Geochemistry and Lithogeochemical Exploration for a Concealed Kimberlite". Goldschmidt Abstracts, 2019, 3676. https://goldschmidtabstracts.info/abstracts/abstractView?id=2019003760

Yin, H., Niu, J., Ren, Y., Cong, J., Zhang, X., Fan, F., Xiao, Y., Zhang, X., Deng, J., Xie, M., He, Z., Zhou, J., Liang, Y., and X. Liu (2015). "An integrated insight into the response of sedimentary microbial communities to heavy metal contamination." Scientific Reports, 5(14266). doi: 10.1038/srep14266

Zhang, B., X. Wang, R. Ye, J. Zhou, H. Liu, D. Liu, Z. Han, X. Lin and Z. Wang (2015). "Geochemical exploration for concealed deposits at the periphery of the Zijinshan copper–gold mine, southeastern China." Journal of Geochemical Exploration 157: 184-193. doi: 10.1016/j.gexplo.2015.06.015

Zhou, J., Z. He, Y. Yang, Y. Deng, S. G. Tringe and L. Alvarez-Cohen (2015). "High-throughput metagenomic technologies for complex microbial community analysis: open and closed formats." MBio 6(1): e02288-02214. doi: 10.1128/mBio.02288-14

Appendix 1

Deerhorn microbiology sample index and geochemistry

Sample_ID	UTM E	UTM N	As ppm	Cu ppm	Mo ppm	K %	C organic %
154303	610775.313	5793143.22	3.38	15.65	0.58	0.11	0.55
154304	610800.175	5793115.03	3.06	75.1	0.3	0.16	1.39
154305	610820.54	5793059.11	3.02	48.4	0.26	0.18	0.52
154306	610859.704	5793032.35	1.72	9.45	0.25	0.09	0.17
154307	610881.139	5792989.62	1.49	8.04	0.18	0.09	0.22
154308	610911.914	5792956.56	1.85	11.55	0.29	0.08	0.22
154309	610950.318	5792918.11	3.35	25.8	0.27	0.17	0.37
154310	610978.608	5792869.04	2.63	36.3	0.29	0.13	1.35
154322	611007.185	5792832.59	2.03	12	0.52	0.1	0.3
154324	611047.292	5792794.36	2.43	11.85	0.47	0.1	0.39
154325	611066.036	5792775.31	1.7	9.32	0.53	0.11	0.39
154326	611112.348	5792724.24	2.29	10.65	0.46	0.07	0.31
154327	611140.4	5792685.92	2.18	13.75	0.45	0.1	0.76
154328	611176.585	5792650.2	1.48	8.29	0.36	0.07	0.24
154329	611199.647	5792596.01	4.72	22.3	0.56	0.13	0.49
154330	611230.676	5792567.04	4.82	15.55	0.64	0.09	0.91
154331	611278.486	5792510.25	2.68	18.45	0.27	0.1	0.65
154332	611292.658	5792492.21	2.39	9.54	0.41	0.09	0.6
154333	611326.194	5792442.89	2.88	9.28	0.4	0.08	0.21
154334	611354.932	5792414.61	2.74	11.35	0.39	0.15	0.16
154335	611394.968	5792369.7	3.62	13.65	0.44	0.13	0.21
154336	611432.261	5792335.49	2.54	15.3	0.33	0.12	0.56
154337	611460.759	5792292.74	2.93	12.25	0.4	0.09	0.22
154338	611494.985	5792253.27	3.61	13.75	0.52	0.09	0.28
154339	611508.871	5792222.8	1.99	9.9	0.39	0.08	0.39
154340	611554.096	5792185.06	2.93	9.45	0.37	0.08	0.53
154348	611585.859	5792143.86	2.71	11.9	0.51	0.09	0.38
154347	611614.338	5792102.03	2.42	14.3	0.53	0.08	0.5
154346	611651.583	5792060.04	3.6	19.8	0.6	0.12	0.25
154345	611675.662	5792026.64	4.31	25.1	0.77	0.08	0.29
154343	611708.704	5791984.36	2.68	13.6	0.48	0.08	0.19
154342	611733.645	5791958.22	1.7	11.4	0.24	0.12	0.22
154341	611775.209	5791916.51	2.12	10.55	0.45	0.09	0.28
154377	611807.784	5791869.77	2.78	15.6	0.4	0.08	0.44
154376	611844.994	5791829.44	2.95	28.8	0.65	0.07	0.4
154375	611870.108	5791790.69	4.59	36	1.19	0.09	0.86
154374	611891.991	5791753.91	4.53	67.7	0.93	0.08	0.93
154373	611931.309	5791721.04	2.18	14.25	0.95	0.08	1.14
154372	611961.335	5791681.48	2.23	18.4	6.41	0.04	26.5
154371	611985.414	5791638.26	1.6	8.67	6.43	0.01	25.8
154370	612027.231	5791600.63	2.38	111	1.56	0.03	23.2
154369	612058.034	5791562.01	1.04	41.1	5.19	0.02	26.9
154368	612095.435	5791538.57	3.61	17.8	0.67	0.17	0.57
154367	612123.701	5791481.34	3.33	88.2	0.45	0.1	0.77

Sample_ID	UTM E	UTM N	As ppm	Cu ppm	Mo ppm	K %	C organic %
154365	612156.001	5791447.03	3.02	18.3	0.62	0.17	1.04
154364	612189.552	5791407.73	3.25	26.1	0.77	0.12	0.65
154363	612211.785	5791370.77	2.84	25	0.53	0.11	0.93
154362	612244.111	5791335.34	4.47	19.6	0.75	0.2	0.35
154361	612278.203	5791292.35	5.22	16.6	0.69	0.14	0.72
154360	612321.736	5791269.6	4.18	11.2	0.55	0.13	0.89
154311	610614.93	5793015.74	1.29	6.61	0.32	0.08	0.34
154312	610634.847	5792974.64	2.2	11.35	0.39	0.09	0.34
154313	610656.186	5792925.97	2	11.45	0.42	0.1	0.25
154314	610692.843	5792909.55	3.26	10.5	0.63	0.11	0.35
154315	610731.738	5792854.23	1.17	10.4	0.12	0.14	0.34
154316	610755.638	5792818.23	1.81	12.55	0.49	0.14	0.39
154317	610804.278	5792790.02	1.84	12	0.45	0.1	0.52
154318	610817.343	5792750.25	2.05	10.9	0.43	0.09	0.37
154319	610857.635	5792713.88	2.21	11.75	0.41	0.12	0.26
154320	610890.039	5792674.18	2.65	13.85	0.5	0.1	0.55
154321	610919.072	5792642.75	2.44	9.54	0.47	0.09	0.28
154349	610954.881	5792593.29	2.29	15.35	0.37	0.1	1.11
154350	610970.703	5792577.7	2.16	19.4	0.45	0.11	0.49
154351	611023.225	5792513.6	1.64	8.72	0.43	0.08	0.42
154352	611054.361	5792479.8	2.57	12.45	0.59	0.1	0.69
154353	611079.65	5792437.9	1.43	7.03	0.18	0.1	0.29
154354	611106.805	5792399.01	1.43	9.42	0.34	0.07	0.37
154355	611144.12	5792358.68	1.98	10.7	0.28	0.09	0.37
154356	611169.276	5792322.71	2.11	10.6	0.41	0.07	0.3
154357	611206.36	5792282.56	3.91	15.3	0.5	0.09	0.61
154358	611240.921	5792243.28	2.64	11.25	0.48	0.08	0.34
154359	611273.033	5792206.72	2.43	9.51	0.39	0.07	0.3
154378	611322.539	5792170.75	2.97	10.15	0.44	0.1	0.31
154379	611331.989	5792119.96	2.52	9.25	0.47	0.08	0.35
154380	611364.968	5792095.48	2.62	9.14	0.43	0.08	0.3
154381	611401.245	5792050.86	4.15	13.8	0.48	0.08	0.49
154395	611418.706	5792018.25	6.04	60.6	0.54	0.08	0.24
154396	611460.558	5791978.76	3.17	43	0.36	0.07	0.2
154397	611484.326	5791949.07	4.48	226	0.25	0.14	0.48
154398	611521.772	5791903.18	3.73	49.6	0.88	0.09	0.76
154399	611550.158	5791860.42	3.67	19.95	0.57	0.11	0.33
154400	611595.416	5791821.38	2.81	15.3	0.55	0.12	0.31
154401	611607.184	5791784	2.14	13	0.5	0.09	0.3
154402	611650.74	5791739.73	4.92	78.5	0.34	0.16	1.63
154407	611613.892	5791683.45	2.22	16.45	0.34	0.06	0.22
154403	611682.524	5791697.8	2.14	17.75	0.53	0.14	0.84
154406	611694.594	5791677.3	2.34	20.6	0.31	0.1	0.43
154404	611704.246	5791663.05	4.36	37.7	0.43	0.08	0.99
154405	611743.029	5791628.69	36.3	235	1.53	0.04	0.65
154394	611780.778	5791586.82	12.6	507	2.3	0.06	0.59
154393	611816.04	5791552.19	8.96	295	1.65	0.07	0.46
154392	611848.29	5791514.9	2.71	18.25	0.75	0.08	0.51

Sample_ID	UTM E	UTM N	As ppm	Cu ppm	Mo ppm	K %	C organic %
154391	611881.944	5791475.98	4.47	23.1	1.03	0.23	0.43
154390	611908.55	5791431.7	4.62	70.4	0.62	0.09	0.61
154389	611939.909	5791393.65	5.08	15.9	0.69	0.1	0.42
154386	611971.664	5791358.21	4.57	10.1	0.51	0.08	0.4
154385	612000.593	5791316.95	5.73	245	0.74	0.08	1.27
154384	612028.381	5791280.86	7.49	37	0.69	0.12	0.89
154383	612067.128	5791241.19	5.22	14	0.46	0.08	0.85
154382	612094.293	5791207.5	4.59	13.85	0.49	0.11	0.6
154408	610484.839	5792927.15	2.45	11.25	0.49	0.07	0.35
154411	610510.917	5792875.06	5.49	29.9	0.67	0.08	0.32
154412	610548.424	5792820.64	2.14	28.3	0.43	0.08	0.58
154413	610571.876	5792794.45	1.98	12.4	0.54	0.07	0.69
154414	610604.899	5792762.55	1.05	8.78	0.32	0.09	0.22
154415	610652.906	5792782.92	1.12	9.01	0.41	0.09	0.41
154416	610660.728	5792697.78	1.85	8.94	0.36	0.08	0.29
154417	610716.129	5792672.5	0.97	8.88	0.35	0.07	0.34
154418	610709.284	5792602.25	1.7	9.75	0.48	0.09	0.34
154419	610754.824	5792565.25	3.01	13.7	0.37	0.09	0.42
154420	610792.905	5792526.05	2.56	10	0.46	0.08	0.2
154421	610813.991	5792493.88	2.8	7.76	0.28	0.08	0.11
154422	610859.725	5792453.36	3.12	10.2	0.34	0.06	0.13
154423	610879.085	5792422.08	3.43	11.35	0.37	0.09	0.27
154438	610895.863	5792358.85	2.98	17.35	0.55	0.11	0.54
154439	610946.338	5792335.32	2.8	10.45	0.43	0.08	0.34
154440	610981.002	5792296.41	4.28	14.45	0.48	0.08	0.56
154441	611016.406	5792265.12	2.45	17.9	0.81	0.1	0.81
154442	611066.604	5792223.59	2.52	12.6	0.5	0.12	0.27
154443	611079.71	5792182.16	4.16	58.5	0.81	0.08	0.45
154444	611121.585	5792151.57	3.53	14.3	0.53	0.09	0.24
154445	611141.727	5792105.85	2.62	14.4	0.62	0.1	0.3
154446	611173.309	5792072.62	1.4	10.35	0.33	0.12	0.51
154447	611189.492	5792020.87	0.83	7.27	0.33	0.07	0.34
154463	611233.805	5791998.32	2.14	14.5	0.41	0.11	0.49
154448	611212.357	5791975.58	1.68	10.65	0.34	0.09	0.26
154462	611278.5	5791943.69	4.82	23.3	0.47	0.12	0.55
154449	611238.715	5791931.85	2.52	11.95	0.4	0.09	0.35
154461	611302.216	5791916.22	1.97	16.45	0.19	0.11	0.37
154450	611265.898	5791886.84	2.06	11.9	0.37	0.08	0.49
154460	611325.759	5791881.32	3.54	18.45	0.3	0.1	0.26
154459	611355.743	5791828.22	1.14	9.45	0.39	0.11	0.32
154458	611383.373	5791819.01	1.39	10.8	0.51	0.1	0.48
154457	611442.811	5791776.77	2	8.99	0.41	0.07	0.16
154456	611465.778	5791717.01	1.85	14.9	0.39	0.08	0.18
154455	611504.506	5791695.08	2.1	14.95	0.43	0.08	0.22
154452	611525.464	5791633.61	6.55	54.1	0.97	0.1	0.38
154451	611551.523	5791613.42	5.84	70.9	0.88	0.1	0.41
154437	611593.166	5791563.18	2.48	20.7	0.72	0.11	0.38
154436	611625.608	5791522.37	4.46	17.65	1.08	0.14	0.58

Sample_ID	UTM E	UTM N	As ppm	Cu ppm	Mo ppm	K %	C organic %
154435	611645.958	5791487.96	3.92	31.5	0.79	0.14	0.66
154434	611683.065	5791452.27	3.87	25.2	0.81	0.12	0.52
154433	611712.538	5791411.95	3.34	16.75	0.67	0.1	0.5
154430	611743.812	5791382.61	4.6	32.4	0.78	0.12	0.44
154429	611775.703	5791331.03	2.84	13.45	0.48	0.09	0.54
154428	611810.504	5791301.78	5.71	37	0.36	0.07	0.85
154427	611844.756	5791251.55	3.43	37.4	0.62	0.12	0.86
154426	611881.053	5791216.58	2.7	14.6	0.45	0.12	0.32
154425	611908.217	5791177.88	4.38	14.95	0.45	0.08	0.47
154424	611955.004	5791137.02	4.36	30.5	0.44	0.08	0.61

Appendix 2

HVC microbiology sample index and geochemistry

Sample ID	UTM E	UTM N	Mo (ppm)	Cu (ppm)	Ag (ppb)	Bi (ppm)
HVC_RC15_001	639660	5587864	0.66	27.64	16	0.1
HVC_RC15_002	639649	5587874	0.98	37.75	14	0.09
HVC_RC15_004	639709	5587877	0.29	12.67	34	0.06
HVC_RC15_005	639766	5587885	7.41	99.74	15	0.1
HVC_RC15_006	639825	5587918	8.35	21.62	7	0.07
HVC_RC15_007	639897	5587929	4.58	50.64	11	0.11
HVC_RC15_008	639952	5587947	3.28	91.51	7	0.13
HVC_RC15_009	639991	5587972	4.71	47.54	21	0.11
HVC_RC15_010	640040	5587977	5.36	57.38	11	0.1
HVC_RC15_011	640079	5587989	8.04	112.7	6	0.08
HVC_RC15_012	640137	5588003	13.98	71.62	15	0.09
HVC_RC15_013	640225	5588038	20.04	193.66	16	0.18
HVC_RC15_014	640275	5588064	2.77	668.87	131	0.11
HVC_RC15_015	640165	5588033	3.36	68.54	7	0.06
HVC_RC15_016	640317	5588091	19.87	1392.47	73	0.22
HVC_RC15_017	640379	5588116	34.8	229.33	13	0.21
HVC_RC15_018	640454	5588184	7.7	273.23	58	0.18
HVC_RC15_019	640439	5588147	11.19	274.19	9	0.2
HVC_RC15_020	640408	5588123	30.8	168	16	0.17
HVC_RC15_022	640492	5588180	16.79	307.94	44	0.27
HVC_RC15_023	640537	5588176	9.23	185.2	112	0.21
HVC_RC15_024	640553	5588201	14.76	360.23	51	0.38
HVC_RC15_026	640582	5588210	14.8	317.42	52	0.35
HVC_RC15_027	640604	5588213	8.67	257.9	38	0.28
HVC_RC15_028	640636	5588219	16.2	305.42	87	0.23
HVC_RC15_029	640677	5588229	22.23	580.81	106	0.45
HVC_RC15_030	640715	5588235	6.95	651.61	63	0.29
HVC_RC15_031	640738	5588282	20.8	184.92	45	0.12
HVC_RC15_032	640792	5588289	8.55	124.98	20	0.1
HVC_RC15_033	640840	5588300	5.41	58.36	30	0.09
HVC_RC15_034	640887	5588327	7.89	110.04	17	0.08
HVC_RC15_035	640940	5588351	3.9	40.06	7	0.05
HVC_RC15_036	640984	5588373	5.63	51.93	5	0.07
HVC_RC15_037	641040	5588396	9.1	107.73	13	0.12
HVC_RC15_038	641094	5588422	10.13	67.56	21	0.11
HVC_RC15_039	641127	5588453	7.16	86.09	15	0.11
HVC_RC15_040	641160	5588474	3.75	49.02	11	0.1
HVC_RC16_001	640133	5588024	7.82	84.92	13	0.11

Sample ID	UTM E	UTM N	Mo (ppm)	Cu (ppm)	Ag (ppb)	Bi (ppm)
HVC_RC16_002	640133	5588023	8.41	77.3	24	0.11
HVC_RC16_004	640157	5588060	5.47	132.4	47	0.17
HVC_RC16_005	640199	5588103	7.73	104.27	7	0.15
HVC_RC16_006	640320	5588121	11.03	206.58	33	0.15
HVC_RC16_007	640345	5587798	2.61	51.02	9	0.09
HVC_RC16_008	640411	5587757	2.29	48.86	14	0.09
HVC_RC16_009	640440	5587823	4.55	98.13	50	0.18
HVC_RC16_010	640457	5587821	5.68	376.5	121	0.29
HVC_RC16_011	640508	5587838	4.63	232.61	16	0.17
HVC_RC16_012	640537	5587839	7.97	149.89	32	0.15
HVC_RC16_013	640578	5587847	6.06	99.97	26	0.12
HVC_RC16_014	640607	5587841	10.67	378.05	70	0.16
HVC_RC16_015	640636	5587874	9.27	400.2	135	0.24
HVC_RC16_016	640676	5587896	8.13	441.3	82	0.25
HVC_RC16_017	640703	5587910	6.73	103.14	37	0.2
HVC_RC16_018	640729	5587960	3.76	173.59	57	0.2
HVC_RC16_019	640758	5587968	3.5	232.62	224	0.7
HVC_RC16_020	640796	5587988	11.75	241.13	119	0.31
HVC_RC16_021	640827	5587995	10.88	576.83	92	0.59
HVC_RC16_022	640859	5588011	27.71	189.64	70	0.19
HVC_RC16_023	640882	5588024	18.02	159.69	16	0.15
HVC_RC16_024	640885	5588019	23.16	208.33	48	0.19
HVC_RC16_026	640917	5588036	23.92	154.93	24	0.18
HVC_RC16_027	640953	5588047	5.38	171.38	12	0.13
HVC_RC15_044	639863	5587309	2.82	102.67	32	0.1
HVC_RC15_045	639901	5587321	3.65	44.29	52	0.11
HVC_RC15_048	639932	5587320	1.57	60.69	24	0.07
HVC_RC15_049	639975	5587321	2.78	20.37	17	0.06
HVC_RC15_050	640023	5587349	2.45	38.78	13	0.13
HVC_RC15_051	640063	5587373	6.65	27.97	8	0.08
HVC_RC15_052	640088	5587388	7.77	26.75	14	0.1
HVC_RC15_053	640134	5587404	3.44	37.56	6	0.1
HVC_RC15_054	640169	5587416	1.57	54.03	8	0.17
HVC_RC15_055	640214	5587424	2.22	49.56	9	0.1
HVC_RC15_057	640304	5587464	5.12	50.66	5	0.16
HVC_RC15_058	640335	5587480	2.91	53.2	9	0.16
HVC_RC15_059	640382	5587475	2.42	40.07	35	0.11
HVC_RC15_060	640414	5587495	1.62	31.49	14	0.11
HVC_RC15_061	640445	5587495	6.75	90.57	24	0.18
HVC_RC15_062	640467	5587500	51.34	232.71	38	0.23
HVC_RC15_063	640501	5587524	3.55	24.09	5	0.1
HVC_RC15_064	640537	5587525	2.33	36.52	8	0.08

Sample ID	UTM E	UTM N	Mo (ppm)	Cu (ppm)	Ag (ppb)	Bi (ppm)
HVC_RC15_065	640546	5587544	2.75	48.1	13	0.12
HVC_RC15_066	640584	5587534	3.67	352.02	23	0.12
HVC_RC15_067	640613	5587551	4.15	242.48	15	0.2
HVC_RC15_070	640633	5587553	7	676.2	190	0.23
HVC_RC15_071	640645	5587563	4.24	403.87	74	0.21
HVC_RC15_072	640663	5587578	3.62	271.7	45	0.17
HVC_RC15_073	640681	5587587	2.69	136.52	15	0.18
HVC_RC15_074	640698	5587600	3.71	115.41	20	0.17
HVC_RC15_075	640714	5587616	7.66	124.42	17	0.17
HVC_RC15_076	640736	5587626	5.58	107.91	21	0.14
HVC_RC15_077	640762	5587639	5.26	56.52	12	0.13
HVC_RC15_078	640775	5587660	3.68	76.06	15	0.15
HVC_RC15_079	640789	5587676	4.46	90.57	21	0.18
HVC_RC15_080	640801	5587697	5.61	140.65	31	0.22
HVC_RC15_081	640814	5587704	3.84	103.05	39	0.22
HVC_RC15_082	640830	5587727	10.73	275.82	52	0.24
HVC_RC15_083	640859	5587727	9.93	54.15	41	0.24
HVC_RC15_084	640892	5587768	10.31	318.9	42	0.52
HVC_RC15_085	640904	5587788	9.77	203.36	150	0.33
HVC_RC15_086	640889	5587724	2.65	97.8	39	0.21
HVC_RC15_087	640937	5587781	10.63	212.45	82	0.31
HVC_RC15_088	640959	5587791	5.35	168.88	27	0.32
HVC_RC15_089	640968	5587814	15.15	152.03	54	0.3
HVC_RC15_090	640981	5587840	8.65	1928.48	211	0.39
HVC_RC15_093	641057	5587882	7.44	185.73	45	0.26
HVC_RC15_094	641113	5587895	9.62	212.78	44	0.29
HVC_RC15_096	641156	5587923	11.71	235.34	31	0.36
HVC_RC15_097	641191	5587967	11.09	130.75	38	0.2
HVC_RC15_098	641230	5587972	6.95	184.5	87	0.24
HVC_RC15_099	641284	5587985	15.15	117.47	32	0.38
HVC_RC15_100	641328	5587995	31.71	483.82	82	0.49
HVC_RC15_101	641371	5588031	5.54	92.68	25	0.13
HVC_RC15_102	641408	5588034	12.28	105.69	30	0.14
HVC_RC15_103	641450	5588045	46.23	924.98	253	0.36